exacerbate human allergic and inflammatory diseases, such as asthma (Rossi *et al.*, 1998) and acute respiratory distress syndrome (Donnelly *et al.*, 1997).

We recently reported excessive expression of MIF mRNA and protein in inflammatory skin lesions and in sera from AD patients (Shimizu *et al.*, 1999; Shimizu, 2005). We also showed that the serum MIF levels decrease as the clinical features of this disease improve, thus suggesting that MIF has a pivotal role in the inflammatory response in AD (Shimizu *et al.*, 1997). These studies raise the possibility that MIF is an important component of Th2-mediated immunopathology in general, and might therefore be relevant to chronic inflammatory allergic conditions.

Eosinophils may aggravate the inflammatory response in the skin of AD patients. Spergel *et al.* (1998, 1999) reported a murine model of allergic skin inflammation elicited by epicutaneous sensitization with ovalbumin (OVA). This model displays many of the features of human AD, including elevated total and specific IgE, dermatitis characterized by infiltration of the dermis by $CD4^+$ T cells and eosinophils, and increased local expression of mRNAs for the cytokines IL-4, IL-5, and IFN-γ. In our present study, MIF transgenic (Tg) mice and MIF knockout (KO) mice were used to assess the potential role of MIF in the pathogenesis of AD in this murine model of allergic skin inflammation. We also investigated the effects of MIF on eotaxin expression of dermal fibroblasts.

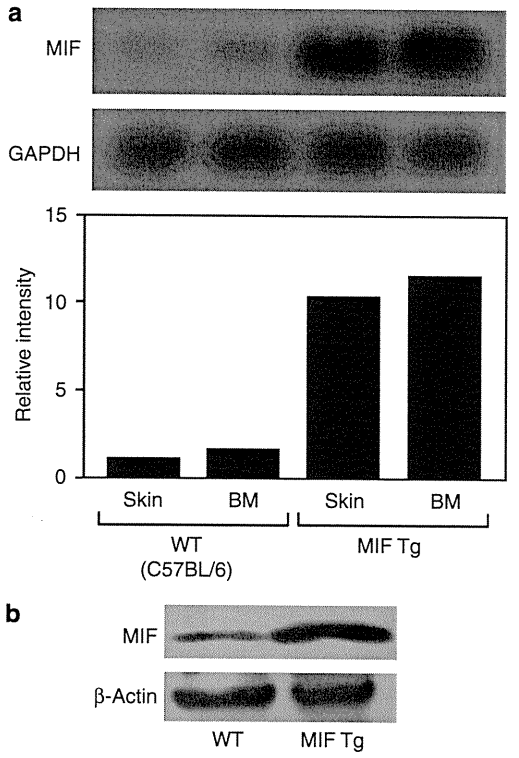

Figure 1. Expression of macrophage migration inhibitory factor (MIF) in tissues from MIF transgenic (Tg) mice. (**a**) Bone marrow (BM) and skin specimens were harvested from MIF Tg and wild-type (WT) mice, and the total RNA levels were determined by northern blot analysis as described in the Materials and Methods. The density of MIF bands was normalized to the glyceraldehyde-3-phosphate dehydrogenase (GAPDH) signals. BM and skin from MIF Tg mice showed an ~10-fold higher level of MIF mRNA expression than those from WT mice. (**b**) Western blot analysis of skin from MIF Tg mice showed that the MIF protein level was also higher in MIF Tg mice than in WT mice.

RESULTS

The expression of MIF was increased in bone marrow and skin from MIF Tg mice

MIF Tg mice exhibited no lethal or prominent pathological lesions in the organs examined. A northern blot analysis revealed the MIF mRNA expression in bone marrow and skin from MIF Tg mice to be ~10 times higher than that in wild-type (WT) mice (Figure 1a). MIF protein was also increased in the skin from MIF Tg mice compared with that from WT mice, as demonstrated by western blotting (Figure 1b).

OVA-sensitized skin sites of MIF Tg mice showed marked eosinophil infiltration

To examine the role of MIF in eosinophilic infiltration, MIF Tg and WT mice were subjected to epicutaneous OVA sensitization. Only a few eosinophils were present in saline-sensitized skin from MIF Tg and WT mice, while eosinophilic infiltration of the dermis was significantly increased following epicutaneous sensitization with OVA. The mean number of eosinophils after OVA sensitization was 13.6 ± 2.84 in MIF Tg mice, but only 4.8 ± 1.37 in WT mice ($P<0.001$; Figure 2a). Figure 2b shows the histological features of OVA-sensitized skin sites in MIF Tg and WT mice. The epidermis was slightly thickened, and numerous eosinophils and mononuclear cells infiltrated the upper dermis around the vessels, in the OVA-sensitized skin of MIF Tg mice.

Eosinophil numbers were not increased in the OVA-sensitized skin of MIF KO mice

To further clarify the roles of MIF in eosinophilic infiltration, MIF KO mice were subjected to epicutaneous OVA sensitization. The mean number of eosinophils after OVA sensitization was 2.0 ± 0.94 in MIF KO mice, and did not differ from that after saline sensitization. Furthermore, this value was significantly lower than that of WT mice (4.8 ± 1.37, $P<0.05$; Figure 3a). Histological features also confirmed only a few eosinophils to be present in the dermis after OVA sensitization in MIF KO mice (Figure 3b).

The expression of eotaxin and Th2-type cytokines increased in the OVA-sensitized skin of MIF Tg mice, but decreased in the OVA-sensitized skin in MIF KO mice

We next examined the expression of mRNAs for eotaxin and cytokines in OVA-sensitized skin specimens from MIF Tg, MIF KO, and WT mice. The expression levels of eotaxin and Th2-type cytokines, especially IL-5, were increased in the OVA-sensitized skin of MIF Tg mice compared with WT mice. However, IFN-γ, a Th1-type cytokine, did not differ between MIF Tg and WT mice. Conversely, low eotaxin mRNA expression was observed in the OVA-sensitized skin of MIF KO mice compared with WT mice. Similarly, the mRNA expression of the Th2-type cytokines, including IL-4,

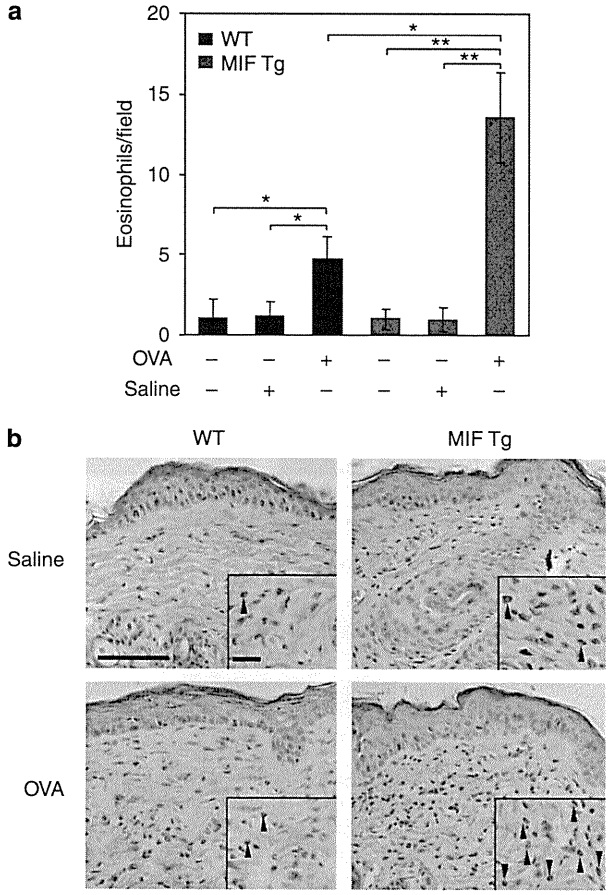

Figure 2. Eosinophil infiltration into ovalbumin (OVA)-sensitized skin sites of macrophage migration inhibitory factor (MIF) transgenic (Tg) mice. (**a**) The number of eosinophils in OVA-sensitized skin sites of MIF Tg mice was compared with the wild-type (WT) mice. Each value represents the mean ± SD ($n=5$; $^*P<0.001$, $^{**}P<0.0001$). (**b**) Histological features of OVA-sensitized skin sites in MIF Tg mice and WT mice. Scale bar for large panels = 50 μm; scale bar for small panels = 10 μm; hematoxylin and eosin section. Arrowheads point to eosinophils. The experiments were repeated three times and similar results were obtained.

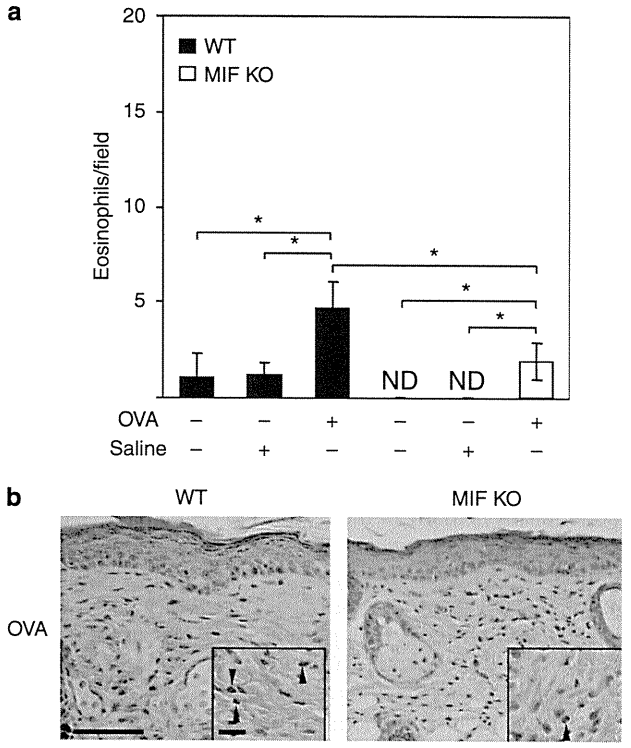

Figure 3. Eosinophil infiltration induced in ovalbumin (OVA)-sensitized skin sites of macrophage migration inhibitory factor (MIF) knockout (KO) mice. (**a**) The number of eosinophils in OVA-sensitized skin sites of MIF KO mice was compared with wild-type (WT) mice. Each value represents the mean ± SD ($n=5$, $^*P<0.05$). (**b**) Histological features of OVA-sensitized skin sites in MIF KO and WT mice. Scale bar for large panels = 50 μm; scale bar for small panels = 10 μm; hematoxylin and eosin section. Arrowheads point to eosinophils. The experiments were repeated three times and similar results were obtained each time.

IL-5, and IL-13, were low in the OVA-sensitized skin of MIF KO mice compared with WT mice (Figure 4).

The expression and production of eotaxin in cultured fibroblasts from MIF Tg mice and from MIF KO mice

To clarify the role of MIF in the expression of eotaxin, we performed *in vitro* experiments. A previous report described that IL-4 could dose-dependently induce the expression of eotaxin mRNA in dermal fibroblasts from humans and mice (Mochizuki *et al.*, 1998). Using this protocol, we analyzed the eotaxin expression in cultured fibroblasts from MIF Tg, MIF KO, and WT mice by stimulating them with IL-4. Unstimulated fibroblasts from these mice barely expressed eotaxin mRNA. However, fibroblasts from MIF Tg mice showed dramatically increased eotaxin mRNA after stimulation with 5 ng ml^{-1} of IL-4 (Figure 5a). To evaluate whether there was an accompanying change in eotaxin protein production, the amount of eotaxin in fibroblast supernatants was also analyzed. Eotaxin proteins in the culture supernatant of fibroblasts from MIF Tg mice were also significantly increased compared with those from WT mice ($^*P<0.005$). However, fibroblasts from MIF KO mice showed minimal expression of eotaxin mRNA even when stimulated with 10 ng ml^{-1} of IL-4. Eotaxin production in the culture supernatant of fibroblasts from MIF KO mice was barely detectable (Figure 5b).

Recombinant MIF restored the expression and production of eotaxin in dermal fibroblasts from MIF KO mice

In dermal fibroblasts from WT mice, stimulation with IL-4 significantly induced the expression of eotaxin mRNA compared with unstimulated fibroblasts (Figure 6a). Addition of recombinant MIF significantly enhanced this increase in eotaxin expression. This suggests that the eotaxin expression in dermal fibroblasts from MIF Tg mice was markedly increased by IL-4 stimulation. A significant amount of eotaxin was also produced by combined stimulation with IL-4 ($^*P<0.005$, $^{**}P<0.05$; Figure 6b). Although the fibroblasts from MIF KO mice showed minimal induction of eotaxin mRNA expression in response to stimulation with IL-4, both the expression of eotaxin mRNA and the production of eotaxin protein were restored by addition of recombinant MIF

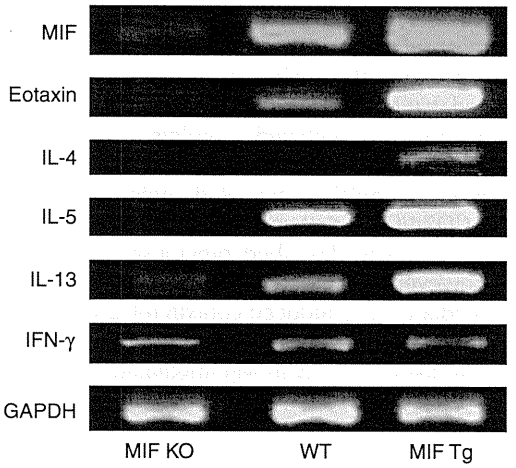

Figure 4. Expression levels of eotaxin and Th2-type cytokines in ovalbumin (OVA)-sensitized skin from macrophage migration inhibitory factor (MIF) transgenic (Tg) mice and MIF knockout (KO) mice. Reverse transcriptase-PCR analyses of eotaxin, IL-4, IL-5, IL-13, and IFN-γ levels in skin sites of MIF Tg and WT mice sensitized with OVA were performed. Eotaxin, IL-4, IL-5, and IL-13 mRNA expression levels were increased in OVA-sensitized MIF Tg; however, both eotaxin and Th2-type cytokines were markedly decreased in OVA-sensitized MIF KO mice, compared with WT mice. The experiments were repeated three times and similar results were obtained. GAPDH, glyceraldehyde-3-phosphate dehydrogenase.

(Figure 6a and b). The levels of eotaxin production in MIF KO mouse fibroblasts exposed to MIF were similar to the levels in WT fibroblasts stimulated with IL-4 (Figure 6b).

DISCUSSION

There is growing evidence that the eosinophil is an important effecter cell in allergic inflammatory diseases, such as asthma and AD. Accumulation of eosinophils in the skin is characteristic of inflammation associated with AD (Leiferman, 1989; Kapp, 1995). This study explored, for the first time, the significant increase in eosinophil infiltration in the skin of MIF Tg mice after OVA sensitization, compared with WT mice. However, in MIF KO mice, eosinophils failed to infiltrate the skin after repeated epicutaneous sensitization with OVA. Eosinophils accumulate at inflammatory sites and release numerous mediators capable of initiating and maintaining allergic inflammation. Yamaguchi *et al.* (2000) reported eosinophils to be an important source of MIF in allergic inflammatory diseases. The number of eosinophils was reported to be significantly decreased in lung tissue and in bronchoalveolar lavage fluid from MIF KO mice after stimulation with OVA, compared with those from WT mice (Mizue *et al.*, 2005; Magalhães *et al.*, 2007; Wang *et al.*, 2009). In an allergic rhinitis model, eosinophil recruitment into the nasal submucosa was also suppressed in MIF KO mice (Nakamaru *et al.*, 2005). Consistent with these findings, our current evidence indicates that MIF is essential for the infiltration of eosinophils into the OVA-sensitized skin.

This study also demonstrated that the expression of both eotaxin and IL-5 is markedly increased in the OVA-sensitized

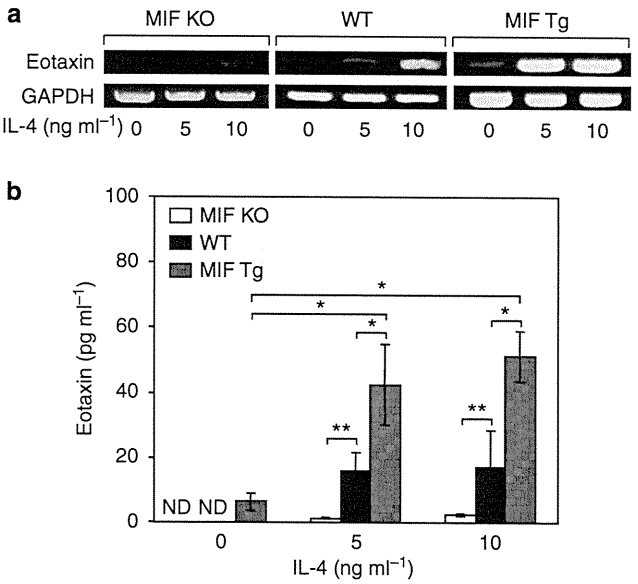

Figure 5. IL-4 induced eotaxin expression and production by fibroblasts from macrophage migration inhibitory factor (MIF) transgenic (Tg) and MIF knockout (KO) mice. Fibroblasts from MIF KO, MIF Tg, and wild-type (WT) mice were stimulated with IL-4 (5 or 10 ng ml^{-1}) for 24 hours. (**a**) RNA was extracted from the cells and the abundance of eotaxin mRNA was evaluated by reverse transcriptase-PCR. Data are from a representative experiment that was repeated three times and yielded similar results. (**b**) The eotaxin content of cultured supernatants was analyzed for eotaxin by ELISA. Each value represents the mean ± SD of five specimens. $*P<0.005$, $**P<0.05$. ND, not detected.

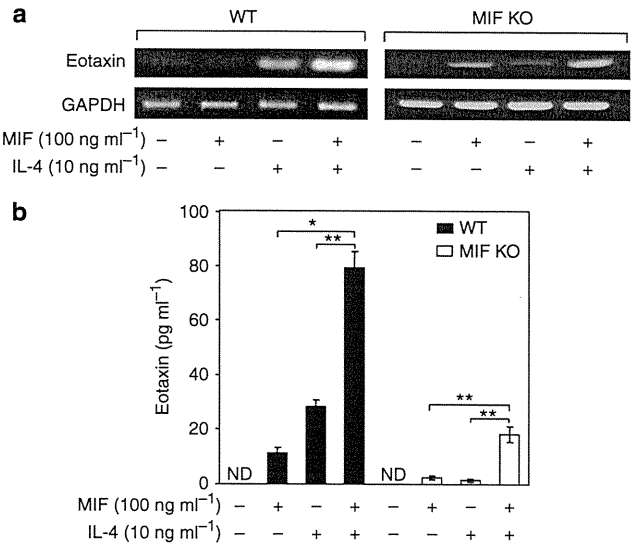

Figure 6. Recombinant macrophage migration inhibitory factor (MIF) restored eotaxin expression and production by IL-4 stimulation in dermal fibroblasts from MIF knockout (KO) mice. The fibroblasts were stimulated with IL-4 (10 ng ml^{-1}), MIF (100 ng ml^{-1}), or both IL-4 and MIF for 24 hours. (**a**) RNA was extracted from cells, and the abundance of eotaxin mRNA was evaluated by reverse transcriptase-PCR. Data are from a representative experiment that was repeated three times showing similar results. (**b**) The eotaxin contents of cultured supernatants were analyzed for eotaxin by ELISA. Each value represents the mean ± SD of six specimens. $*P<0.005$, $**P<0.05$. GAPDH, glyceraldehyde-3-phosphate dehydrogenase; ND, not detected.

skin sites of MIF Tg mice skin. The other Th2-type cytokines, IL-4 and IL-13, were also slightly increased in MIF Tg mice. On the other hand, the expression levels of eotaxin and Th2-type cytokines were markedly decreased in the OVA-sensitized skin sites of MIF KO mice. Acute AD involves a systemic Th2 response with eosinophilia, and marked infiltration of Th2 cells into skin lesions. These infiltrating T cells predominantly express IL-4, IL-5, and IL-13. Furthermore, the roles of cytokines in the induction of migration and the accumulation of eosinophils into an inflamed tissue have been extensively studied in recent years. Some of the important eosinophil chemoattractant cytokines include IL-5, IL-8, eotaxin, RANTES (regulated on activation, normal T cell expressed and secreted), and monocyte chemoattractant protein-3 (Lampinen *et al.*, 2004). Among these, eotaxin (CC chemokine ligand-11) is one of the most important eosinophil-selective chemoattractants (Jose *et al.*, 1994; Garcia-Zepeda *et al.*, 1996). Eotaxin is secreted by several cell types: epithelial cells, fibroblasts, and activated infiltrating leukocytes such as eosinophils (Garcia-Zepeda *et al.*, 1996; Ponath *et al.*, 1996; Uguccioni *et al.*, 1996). Eotaxin is reportedly related to the eosinophilia in allergic diseases, including AD and asthma (Ying *et al.*, 1997; Yawalkar *et al.*, 1999). IL-5 also has an important role in eosinophil development and differentiation (Sanderson, 1992). IL-5 KO mice had virtually no eosinophils in either saline-sensitized skin or in OVA-sensitized skin (Spergel *et al.*, 1999). Recently, Magalhães *et al.* (2009) reported that MIF was involved in IL-5-driven maturation of eosinophils and in tissue eosinophilia associated with *Schistosoma mansoni* infection. In addition, several earlier studies demonstrated that MIF KO mice failed to develop tissue eosinophilia, and that eotaxin, IL-4, and IL-5 were not induced in either allergic lung tissues or bronchoalveolar lavage fluid (Mizue *et al.*, 2005; Wang *et al.*, 2006). Accordingly, our results suggest that MIF is important in regulating both eotaxin and IL-5 in OVA-sensitized inflamed skin tissue.

In support of these *in vivo* observations, this study demonstrated that the expression of eotaxin was significantly increased after stimulation with IL-4 in fibroblasts from MIF Tg mice compared with WT fibroblasts, but not in fibroblasts from MIF KO mice. However, eotaxin expression in fibroblasts from MIF KO mice was restored by addition of recombinant MIF. These observations suggest that MIF is crucial to the expression of eotaxin, and antigen-induced eosinophil infiltration is suspected to be induced by eotaxin mainly by MIF, in addition with IL-5 production involved in MIF. Previous observations have shown that either IL-4 or IL-13 can increase eotaxin expression, and that they function synergistically with proinflammatory cytokines, such as tumor necrosis factor-α, to increase the production of eotaxin in epithelial cells and fibroblasts (Mochizuki *et al.*, 1998; Nakamura *et al.*, 1998; Li *et al.*, 1999; Stellato *et al.*, 1999; Fujisawa *et al.*, 2000; Terada *et al.*, 2000). Increases in both IL-4 and IL-13 in the inflamed skin of MIF Tg mice might involve enhancing the tissue eosinophilia. Furthermore, tumor necrosis factor-α secretion induced by MIF also has the ability to increase eotaxin expression in MIF Tg mice, on the basis of the known capacity of MIF to trigger the secretion of several inflammatory cytokines, including tumor necrosis factor-α (Donnelly *et al.*, 1997). It was recently elucidated that MIF activates an extracellular signal-regulated kinase-1/2–mitogen-activated protein kinase signaling through its receptor CD74 (Leng *et al.*, 2003) and c-Jun N-terminus kinase–mitogen-activated protein kinase signaling through CD74/CXCR4 (Lue *et al.*, 2011), in addition to the endocytic pathway described previously (Kleemann *et al.*, 2000); however, the receptor-mediated mechanism involved in MIF-mediated IL-4-induced eotaxin release is unclear. This mechanism should therefore be an important focus of research in association with MIF-mediated skin allergy.

Finally, we suggest that the inhibition of MIF might be an effective treatment for AD, suppressing both eosinophil infiltration and eotaxin expression in the skin. We recently demonstrated that in murine models of AD, MIF–DNA vaccination elicited the production of endogenous anti-MIF antibodies, producing rapid improvement of AD skin manifestations (Hamasaka *et al.*, 2009). Our previous data and the current findings therefore hold promise for the development of MIF inhibitors as a therapeutic strategy for allergic diseases.

MATERIALS AND METHODS

Materials

The following materials were obtained from commercial sources: a mouse eotaxin-specific ELISA kit from Genzyme TECHNE (Cambridge, MT); Isogen RNA extraction kit from Nippon Gene (Tokyo, Japan); M-MLV reverse transcriptase from GIBCO (Grand Island, NY); Taq DNA polymerase from Perkin-Elmer (Norwalk, CO); nylon membranes from Schleicher & Schuell (Keene, NH); Ficoll-Plaque Plus and Protein A Sepharose from Pharmacia (Uppsala, Sweden); recombinant mouse IL-4 from R&D systems (Minneapolis, MN). Recombinant rat MIF (this recombinant MIF crossreacts with that of mice) was expressed in *Escherichia coli* BL21/DE3 (Novagen, Madison, WI) and was purified as described previously (Shimizu *et al.*, 2004). All other chemicals were of analytical grade.

Mice

The MIF-overexpressing Tg mice were established after complementary DNA microinjection. Physical and biochemical characteristics, including body weight, blood pressure, and serum cholesterol and blood sugar levels, were normal, as reported previously (Sasaki *et al.*, 2004). The transgene expression was regulated by a hybrid promoter composed of the cytomegalovirus enhancer and the β-actin/β-globin promoter, as reported previously (Akagi *et al.*, 1997). The strain of the original MIF Tg mice was ICR, which were backcrossed with C57BL/6 for at least 10 generations. Tg mice were maintained by heterozygous sibling mating. Aged MIF Tg mice of 12 months or older developed neither skin allergies nor diseases. The MIF-deficient (KO) mice were established by targeted disruption of the *MIF* gene as described previously (Honma *et al.*, 2000), using a mouse strain bred onto a C57BL/6 background. MIF Tg, MIF KO, and WT mice were maintained under specific-pathogen-free conditions at the Institute for Animal Experiments of the Graduate School of Medicine and Pharmaceutical Sciences, University of Toyama. All experiments were performed on 8-week-old female adult mice.

Epicutaneous sensitization

Epicutaneous sensitization of mice was performed as described previously (Spergel *et al.*, 1998). Briefly, each mouse was anesthetized with 10% nembutal (Hospira, Osaka, Japan), then shaved with a razor. One hundred mg of OVA (Sigma, St Louis, MO) in 100 μl of normal saline were placed on a 1 × 1 cm patch (Alcare, Tokyo, Japan), which was secured to the skin with a transparent bio-occlusive dressing (ALCARE). The patch was left in place for 1 week and then removed. At the end of the second week, an identical patch was reapplied to the same skin site. Each mouse had a total of three 1-week exposures to the patch, separated from each other by 2-week intervals. Inspection confirmed that the patch was still in place at the end of each sensitization period. Skin biopsies from treated areas were obtained for RNA isolation and histological evaluation. Six-micrometer thick skin sections were stained with hematoxylin and eosin (H&E). Eosinophils were counted under a microscope at a magnification of ×400 and expressed as the mean number of the cells in five random fields (one section per mouse, five mice per group).

Northern blot analysis

Bone marrow cells were isolated from the femurs of MIF Tg or WT mice, and 1×10^6 cells ml^{-1} was collected. Total RNA was isolated from bone marrow cells and skin from mice using an Isogen RNA extraction kit according to the manufacturer's protocols. Twenty μg of RNA from control and test samples were loaded onto a formaldehyde-agarose gel and the RNA was transferred onto a nylon membrane. RNA fragments obtained by restriction enzyme treatment for MIF and glyceraldehyde-3-phosphate dehydrogenase were labeled with [α-^{32}P]deoxycytidine triphosphate using a DNA random primer labeling kit (Enzo Life Sciences International, Farmingdale, NY). Hybridization was carried out at 42 °C for 24–48 hours. Post-hybridization washing was performed in 0.1% SDS with 0.2 × standard saline citrate (1 × standard saline citrate: 0.15 M NaCl, 0.015 M sodium citrate) at 65 °C for 15 minutes. The radioactive bands were visualized by autoradiography on Kodak X-AR5 film (Tokyo, Japan) and quantitatively analyzed using the NIH Image system (Bethesda, MD). The results were normalized by compensating for the glyceraldehyde-3-phosphate dehydrogenase mRNA levels.

Reverse transcription-PCR analysis

Total RNA was extracted from each mouse skin specimen. RNA reverse transcription was performed with M-MLV reverse transcriptase using random hexamer primers and subsequent amplification using Taq DNA polymerase. PCR was carried out for 35–40 cycles with denaturation at 94 °C for 30 seconds, annealing from 46 to 64 °C for 1 minute and extension at 72 °C for 45 seconds using a thermal cycler (PE Applied Biosystems Gene Amp PCR system 9700, Life Technologies Japan, Tokyo, Japan). The primers used in this study are described in Supplementary Table S1 online. After PCR, the amplified products were analyzed by 2% agarose gel electrophoresis.

Western blot analysis

The epidermis of each mouse was homogenized with a Polytron homogenizer (Kinematica, Lausanne, Switzerland). The protein concentrations of the cell homogenates were quantified using a Micro BCA protein assay reagent kit (Thermo Fisher Scientific, Yokohama, Japan). Equal amounts of homogenates were dissolved in 20 μl of Tris-HCL, 50 mM (pH 6.8), containing 2-mercaptoethanol (1%), SDS (2%), glycerol (20%) and bromophenol blue (0.04%), and then were heated to 100 °C for 5 minutes. The samples were then subjected to SDS-PAGE and electrophoretically transferred onto a nitrocellulose membrane. The membranes were blocked with 2.5% non-fat dry milk powder in phosphate-buffered saline, probed with antibodies against MIF (Shimizu *et al.*, 1996) and subsequently reacted with secondary IgG antibodies coupled with horseradish peroxidase. The resultant complexes were processed for the ECL detection system (Amersham Biosciences, Buckinghamshire, UK). The relative amounts of proteins associated with specific antibodies were normalized according to the intensities of β-actin (Sigma).

Cell culture

Skin specimens were obtained from the dorsal surfaces of newborn MIF Tg, MIF KO, and WT mice. The skin specimens were cut into 3–5 mm pieces and placed on a large Petri dish with the subcutaneous side down, followed by tissue incubation for 1 week in a humidified atmosphere of 5% CO_2 at 37 °C. Once sufficient numbers of fibroblasts had migrated out of the skin sections, pieces of the skin were removed and the cells were passaged by trypsin digestion in the same manner as wound-harvested fibroblasts. Fibroblasts were grown in DMEM containing 10% fetal calf serum and 1% penicillin/streptomycin. After 3 passages, the fibroblasts were used for the experiments. The fibroblasts from MIF KO and WT mice were stimulated with MIF (100 ng ml^{-1}), IL-4 (10 ng ml^{-1}), or MIF (100 ng ml^{-1}) in combination with IL-4 (10 ng ml^{-1}) for 24 hours. We also stimulated the fibroblasts from MIF Tg, MIF KO, and WT mice with IL-4 (5 or 10 ng ml^{-1}) alone for 24 hours. The cells were analyzed using reverse transcriptase-PCR. Culture supernatants were analyzed for eotaxin by ELISA.

Statistical analysis

Values are expressed as the means ± SD of the respective test or control group. The statistical significance of differences between the control and test groups was evaluated by either Student's *t*-test or one-way analysis of variance.

CONFLICT OF INTEREST

The authors state no conflict of interest.

ACKNOWLEDGMENTS

This research was supported by a Grant-in-Aid for Scientific Research (Nos.11670813 and 13357008) from the Japan Society for the Promotion of Science.

SUPPLEMENTARY MATERIAL

Supplementary material is linked to the online version of the paper at http://www.nature.com/jid

REFERENCES

Akagi Y, Isaka Y, Akagi A *et al.* (1997) Transcriptional activation of a hybrid promoter composed of cytomegalovirus enhancer and beta-actin/beta-globin gene in glomerular epithelial cells *in vivo*. *Kidney Int* 51:1265–9

Bernhagen J, Calandra T, Bucala R (1998) Regulation of the immune response by macrophage migration inhibitory factor: biological and structural features. *J Mol Med* 76:151–61

Bernhagen J, Calandra T, Mitchell RA *et al.* (1993) MIF is a pituitary-derived cytokine that potentiates lethal endotoxaemia. *Nature* 365:756–9

Bloom BR, Bennett B (1966) Mechanism of reaction *in vivo* associated with delayed-type hypersensitivity. *Science* 153:80–2

Bucala R (1996) MIF re-evaluated: pituitary hormone and glucocorticoid-induced regulator of cytokine production. *FASEB J* 7:19–24

Cheng Q, McKeown SJ, Santos L *et al.* (2010) Macrophage migration inhibitory factor increases leukocyte-endothelial interactions in human endothelial cells via promotion of expression of adhesion molecules. *J Immunol* 185:1238–47

Donnelly SC, Haslett C, Reid PT *et al.* (1997) Regulatory role for macrophage migration Inhibitory factor in acute respiratory distress syndrome. *Nat Med* 3:320–3

Fujisawa T, Kato Y, Atsuta J *et al.* (2000) Chemokine production by the BEAS-2B human bronchial epithelial cells: differential regulation of eotaxin, IL-8, and RANTES by TH2- and TH1-derived cytokines. *J Allergy Clin Immunol* 105:126–33

Garcia-Zepeda EA, Rothenberg ME, Ownbey RT *et al.* (1996) Human eotaxin is a specific chemoattractant for eosinophil cells and provides a new mechanism to explain tissue eosinophilia. *Nat Med* 2:449–56

Gregory JL, Leech MT, David JR *et al.* (2004) Reduced leukocyte-endothelial cell interactions in the inflamed microcirculation of macrophage migration inhibitory factor-deficient mice. *Arthritis Rheum* 50:3023–34

Gregory JL, Morand EF, McKeown SJ *et al.* (2006) Macrophage migration inhibitory factor induces macrophage recruitment via CC chemokine ligand 2. *J Immunol* 177:8072–9

Hamasaka A, Abe R, Koyama Y *et al.* (2009) DNA vaccination against macrophage migration inhibitory factor improves atopic dermatitis in murine models. *J Allergy Clin Immunol* 124:90–9

Honma N, Koseki H, Akasaka T *et al.* (2000) Deficiency of the macrophage migration inhibitory factor gene has no significant effect on endotoxaemia. *Immunology* 100:84–90

Jose PJ, Griffiths-Johnson DA, Collins PD *et al.* (1994) Eotaxin: a potent eosinophil chemoattractant cytokine detected in a guinea pig model of allergic airways inflammation. *J Exp Med* 179:881–7

Kapp A (1995) Atopic dermatitis-the skin manifestation of atopy. *Clin Exp Allergy* 25:210–9

Kleemann R, Hausser A, Geiger R *et al.* (2000) Intracellular action of the cytokine MIF to modulate AP-1 activity and the cell cycle through Jab1. *Nature* 408:211–6

Lampinen M, Carlson M, Hakansson LD *et al.* (2004) Cytokine-regulated accumulation of eosinophils in inflammatory disease. *Allergy* 59:793–805

Leiferman KM (1989) Eosinophils in atopic dermatitis. *Allergy* 44:20–6

Leng L, Metz CN, Fang Y *et al.* (2003) MIF signal transduction initiated by binding to CD74. *J Exp Med* 197:1467–76

Leung DY, Nicklas RA, Li JT *et al.* (2004) Disease management of atopic dermatitis: an updated practice parameter. Joint Task Force on Practice Parameters. *Ann Allergy Asthma Immunol* 93:S1–21

Li L, Xia Y, Nguyen A *et al.* (1999) Effects of Th2 cytokines on chemokine expression in the lung: IL-13 potently induces eotaxin expression by airway epithelial cells. *J Immunol* 162:2477–87

Lue H, Dewor M, Leng L *et al.* (2011) Activation of the JNK signaling pathway by macrophage migration inhibitory factor (MIF) and dependence on CXCR4 and CD74. *Cell Signal* 23:135–44

Magalhães ES, Mourao-Sa DS, Vieira-de-Abreu A *et al.* (2007) Macrophage migration inhibitory factor is essential for allergic asthma but not for Th2 differentiation. *Eur J Immunol* 37:1097–106

Magalhães ES, Paiva CN, Souza HS *et al.* (2009) Macrophage migration inhibitory factor is critical to interleukin-5-driven eosinophilopoiesis and tissue eosinophilia triggered by Schistosoma mansoni infecton. *FASEB J* 23:1262–71

Mizue Y, Ghani S, Leng L *et al.* (2005) Role for macrophage migration inhibitory factor in asthma. *Proc Natl Acad Sci USA* 102:14410–5

Mochizuki M, Bartels J, Mallet AI *et al.* (1998) IL-4 induces eotaxin: a possible mechanism of selective eosinophil recruitment in helminth infection and atopy. *J Immunol* 160:60–8

Morar N, Willis-Owen SA, Moffatt MF *et al.* (2006) The genetics of atopic dermatitis. *J Allergy Clin Immunol* 118:24–34

Nakamaru Y, Oridate N, Nishihira J *et al.* (2005) Macrophage migration inhibitory factor (MIF) contributes to the development of allergic rhinitis. *Cytokine* 31:103–8

Nakamura H, Haley KJ, Nakamura T *et al.* (1998) Differential regulation of eotaxin expression by TNF-alpha and PMA in human monocytic U-937 cells. *Am J Physiol* 275:L601–10

Ponath PD, Qin S, Post TW *et al.* (1996) Molecular cloning and characterization of a human eotaxin receptor expressed selectively on eosinophils. *J Exp Med* 183:2437–48

Roger T, David J, Glauser MP *et al.* (2001) MIF regulates innate immune responses through modulation of Toll-like receptor 4. *Nature* 414:920–4

Rossi AG, Haslett C, Hirani N *et al.* (1998) Human circulating eosinophils secrete macrophage migration inhibitory factor (MIF): potential role in asthma. *J Clin Invest* 15:2869–74

Sanderson CJ (1992) Interleukin-5, eosinophils, and disease. *Blood* 79:3101–9

Sasaki S, Nishihira J, Ishibashi T *et al.* (2004) Transgene of MIF induces podocyte injury and progressive mesangial sclerosis in the mouse kidney. *Kidney Int* 65:469–81

Shimizu T (2005) Role of macrophage migration inhibitory factor (MIF) in the skin. *J Dermatol Sci* 37:65–73

Shimizu T, Abe R, Ohkawara A *et al.* (1997) Macrophage migration inhibitory factor is an essential immunoregulatory cytokine in atopic dermatitis. *Biochem Biophy Res Commun* 240:173–8

Shimizu T, Abe R, Ohkawara A *et al.* (1999) Increased production of macrophage migration inhibitory factor (MIF) by PBMCs of atopic dermatitis. *J Allergy Clin Immunol* 104:659–64

Shimizu T, Nishihira J, Watanabe H *et al.* (2004) Cetirizine, an H1-receptor antagonist, suppresses the expression of macrophage migration inhibitory factor (MIF): its potential anti-inflammatory action. *Clin Exp Allergy* 34:103–9

Shimizu T, Ohkawara A, Nishihira J *et al.* (1996) Identification of macrophage migration inhibitory factor (MIF) in human skin and its immunohistochemical localization. *FEBS Lett* 381:188–202

Spergel JM, Mizoguchi E, Brewer JP *et al.* (1998) Epicutaneous sensitization with protein antigen induces localized allergic dermatitis and hyperresponsiveness to methacholine after single exposure to aerosolized antigen in mice. *J Clin Invest* 101:1614–22

Spergel JM, Mizoguchi E, Oettgen H *et al.* (1999) Roles of TH1 and TH2 cytokines in a murine model of allergic dermatitis. *J Clin Invest* 103:1103–11

Stellato C, Matsukura S, Fal A *et al.* (1999) Differential regulation of epithelial-derived C-C chemokine expression by IL-4 and glucocorticoid budesonide. *J Immunol* 163:5624–32

Terada N, Hamano N, Nomura T *et al.* (2000) Interleukin-13 and tumor necrosis factor-a synergistically induce eotaxin production in human nasal fibroblasts. *Clin Exp Allergy* 20:348–55

Uguccioni M, Loetscher P, Forssmann U *et al.* (1996) Monocyte chemotactic protein 4 (MCP-4), a novel structural and functional analogue of MCP-3 and eotaxin. *J Exp Med* 183:2379–84

Wang B, Huang X, Wolters PJ *et al.* (2006) Cutting edge: deficiency of macrophage migration inhibitory factor impairs murine airway allergic responses. *J Immunol* 177:5779–84

Wang B, Zhang Z, Wang Y *et al.* (2009) Molecular cloning and characterization of macrophage migration inhibitory factor from small abalone Haliotis diversicolor supertexta. *Fish Shellfish Immunol* 27:57–64

Weiser WY, Temple PA, Witek-Giannotti JS *et al.* (1989) Molecular cloning of a cDNA encoding a human macrophage migration inhibitory factor. *Proc Natl Acad Sci USA* 86:7522–6

Yamaguchi E, Nishihira J, Shimizu T *et al.* (2000) Macrophage migration inhibitory factor (MIF) in bronchial asthma. *Clin Exp Allergy* 30:1244–9

Yawalkar N, Uguccioni M, Schärer J *et al.* (1999) Enhanced expression of eotaxin and CCR3 in atopic dermatitis. *J invest Dermatol* 113:43–8

Ying S, Robinson DS, Meng Q *et al.* (1997) Enhanced expression of eotaxin and CCR3 mRNA and protein in atopic athma. Association with airway hyperresponsiveness and predominant co-localization of eotaxin mRNA to bronchial epithelial and endothelial cells. *Eur J Immunol* 27:3507–16

xeroderma pigmentosum skin *in vitro*: a model to study hypersensitivity to UV light. *Photochem Photobiol* 81:19–24

Epp N, Fürstenberger G, Müller K *et al.* (2007) 12R-lipoxygenase deficiency disrupts epidermal barrier function. *J Cell Biol* 177:173–82

Gache Y, Baldeschi C, Del RM *et al.* (2004) Construction of skin equivalents for gene therapy of recessive dystrophic epidermolysis bullosa. *Hum Gene Ther* 15:921–33

García M, Larcher F, Hickerson RP *et al.* (2011) Development of skin-humanized mouse models of pachyonychia congenita. *J Invest Dermatol* 131:1053–60

Green H (1978) Cyclic AMP in relation to proliferation of the epidermal cell: a new view. *Cell* 15:801–11

Lampert IA (1985) Expression of class II MHC antigen on epithelia and autoimmunity. *Lancet* 2:1078

Leigh I, Watt F (1994) *Keratinocyte Methods.* Cambridge: Cambridge University Press

Mildner M, Ballaun C, Stichenwirth M *et al.* (2006) Gene silencing in a human organotypic skin model. *Biochem Biophys Res Commun* 348:76–82

Mildner M, Jin J, Eckhart L *et al.* (2010) Knockdown of filaggrin impairs diffusion barrier function and increases UV sensitivity in a human skin model. *J Invest Dermatol* 130:2286–94

O'Shaughnessy RF, Choudhary I, Harper JI (2010) Interleukin-1 alpha blockade prevents hyperkeratosis in an *in vitro* model of lamellar ichthyosis. *Hum Mol Genet* 19:2594–605

Oji V, Eckl KM, Aufenvenne K *et al.* (2010) Loss of corneodesmosin leads to severe skin barrier defect, pruritus, and atopy: unraveling the peeling skin disease. *Am J Hum Genet* 87:274–81

Rheinwald JG, Green H (1975) Serial cultivation of strains of human epidermal keratinocytes: the formation of keratinizing colonies from single cells. *Cell* 6:331–43

Schäfer-Korting M, Bock U, Diembeck W *et al.* (2008) The use of reconstructed human epidermis for skin absorption testing: results of the validation study. *Altern Lab Anim* 36:161–87

Thomas AC, Tattersall D, Norgett EE *et al.* (2009) Premature terminal differentiation and a reduction in specific proteases associated with loss of ABCA12 in Harlequin ichthyosis. *Am J Pathol* 174:970–8

Tjabringa G, Bergers M, van Rens D *et al.* (2008) Development and validation of human psoriatic skin equivalents. *Am J Pathol* 173: 815–23

Williams ML (1992) Ichthyosis: mechanisms of disease. *Pediatr Dermatol* 9:365–8

AKT Has an Anti-Apoptotic Role in ABCA12-Deficient Keratinocytes

Journal of Investigative Dermatology (2011) **131,** 1942–1945; doi:10.1038/jid.2011.132; published online 2 June 2011

TO THE EDITOR

Harlequin ichthyosis (HI) is a hereditary skin disorder characterized by severe hyperkeratosis and impaired skin barrier function (Moskowitz *et al.*, 2004; Akiyama *et al.*, 2005). We have identified the ATP-binding cassette transporter A12 (*ABCA12*) as the causative gene of HI and, furthermore, demonstrated that ABCA12 is essential for keratinocyte lipid transport (Akiyama *et al.*, 2005; Yanagi *et al.*, 2008). Loss of ABCA12 function causes lipid transport to be defective in keratinocytes of the upper spinous and granular layers, resulting in the deposition of numerous intracellular lipid droplets and malformation of intercellular lipid layers (Akiyama *et al.*, 2005; Yanagi *et al.*, 2010). Recently, we have shown that gangliosides accumulate in the differentiated keratinocytes of HI patients (Mitsutake *et al.*, 2010). On the basis of the evidence that lipid accumulation is involved in keratinocyte apoptosis (Wang *et al.*, 2001; Uchida *et al.*, 2010), we investigated apoptotic and anti-apoptotic parameters in skin samples from HI patients and *Abca12*$^{-/-}$ HI model mice.

We studied the skin of two HI patients and that of *Abca12*$^{-/-}$ mice. The *ABCA12* mutations of the two HI patients have been previously reported: one patient has the homozygous splice acceptor site mutation c.3295-2A>G and the other has the homozygous nonsense mutation p.Arg434X (Akiyama *et al.*, 2005). The procedure for generating *Abca12*$^{-/-}$ mice, the establishment of primary-cultured keratinocytes, immunofluorescence staining, immunoblotting, and real-time reverse transcriptase PCR analysis has been previously described (Yanagi *et al.*, 2008, 2010). First, we investigated the apoptosis of HI patient epidermis by hematoxylin–eosin stain and TUNEL assay (*In situ* Apoptosis Detection Kit, Takara Bio, Otsu, Japan). In the HI patients, the nuclei of the granular-layer keratinocytes were condensed (Figure 1b) and they show positive for TUNEL labeling (Figure 1d), although apoptotic nuclei are rare in the normal human epidermis (Figure 1a, c). The histopathological findings and results of TUNEL staining of the *Abca12*$^{-/-}$ mice were similar to those in the skin of the HI patients (Figure 1f and h). TUNEL staining in the epidermis of 18.5-day embryos indicated that the apoptosis of keratinocytes started during fetal skin development (Figure 1j).

We assessed the degree of AKT activation of *Abca12*$^{-/-}$ skin and keratinocytes using anti-AKT antibody #4691 and anti-phosphorylated AKT (Ser473) #4060 antibody (Cell Signaling, Danvers, MA). By immunoblot analysis, differentiated primary-cultured keratinocytes and the epidermis of *Abca12*$^{-/-}$ mice showed higher expression levels of Ser-473 phosphorylated AKT than those of the control wild-type mice (Figure 1o). Immunofluorescence staining detected phosphorylated AKT in the upper granular-layer keratinocytes of the *Abca12*$^{-/-}$ mouse skin (Figure 1l), but not in the skin of control wild-type mouse (Figure 1k). Cell proliferation was assessed by Ki-67 immunofluorescence (Figure 1). Ki-67 stain was similar in the wild-type and the *Abca12*$^{-/-}$ samples, indicating that the granular-layer keratinocytes of the *Abca12*$^{-/-}$ neonatal mice showed no excessive cell proliferation. To clarify whether AKT activation has

Abbreviations: ABCA12, ATP-binding cassette transporter A12; HI, harlequin ichthyosis; PPAR, peroxisome proliferator-activated receptor; RXR, retinoid X receptor

anti-apoptotic effects on *Abca12*$^{-/-}$ keratinocytes, we performed TUNEL staining of keratinocytes treated with AKT inhibitor, which blocks AKT phosphorylation (#124017; InSolution Akt Inhibitor VIII, Calbiochem, San Diego, CA). *Abca12*$^{-/-}$ keratinocytes incubated with 10 μM #124017 AKT inhibitor showed a notably greater number of TUNEL-positive cells than both wild-type keratinocytes with AKT inhibitor and *Abca12*$^{-/-}$ keratinocytes without AKT inhibitor (Figure 2). These results suggest that AKT activation helps *Abca12*$^{-/-}$ keratinocytes to avoid apoptosis. Furthermore, mRNA and protein levels of peroxisome proliferator-activated receptor (PPAR)-δ from *Abca12*$^{-/-}$ epidermis were shown to be significantly higher than those from wild-type epidermis (Taqman Gene Expression Assay, probe ID, Mm00803184_m1, Mm99999915_g1, Applied Biosystems, Carlsbad, CA; anti-PPAR-δ antibody H-74, Santa Cruz, Santa Cruz, CA; Supplementary Figure S1 online), which suggests upregulation of PPAR-δ as a candidate pathway for AKT activation.

Herein, we have suggested that apoptosis is involved in the pathomechanism of HI. Defective lipid transport due to loss of ABCA12 function leads to the accumulation of intracellular lipids, including glucosylceramides and gangliosides (Akiyama *et al.*, 2005; Mitsutake *et al.*, 2010). Studies by Wang *et al.* (2001) and Sun *et al.* (2002) showed that the elevation of ganglioside levels leads to keratinocyte apoptosis. Thus, we are able to speculate that the accumulation of gangliosides leads to the apoptosis of *Abca12*$^{-/-}$ keratinocytes, although the exact mechanism of apoptosis in *Abca12*$^{-/-}$ keratinocytes remains unclear.

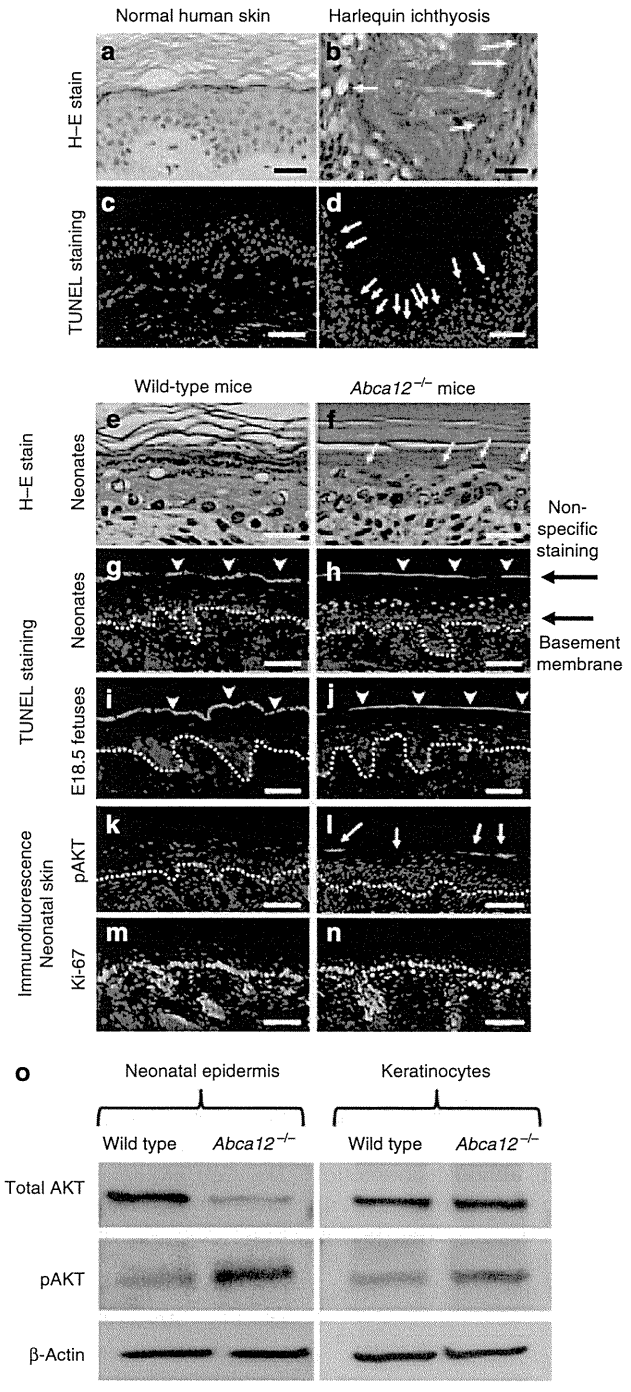

Figure 1. ATP-binding cassette transporter A12-deficient keratinocytes show TUNEL-positive nuclei and AKT activation. (**a**–**d**) In the harlequin ichthyosis patients, the nuclei of the granular-layer keratinocytes are condensed (**b**, white arrows) and they show positive TUNEL labeling (**d**, white arrows), although apoptotic nuclei are rare in the normal human epidermis (**a**, **c**). Data shown are representative of those from the two harlequin ichthyosis patients. (**e**, **f**) Granular-layer keratinocytes of *Abca12*$^{-/-}$ mice show more condensed nuclei (**f**, white arrows) than those of wild-type mice (**e**). (**g**–**j**) Granular-layer keratinocytes of *Abca12*$^{-/-}$ mice, a neonate (**h**) and an 18.5-day embryo (**j**), show TUNEL-positive nuclei. No TUNEL-positive cells are seen in the epidermis of the control wild-type mice (**g**, **i**). Dotted lines indicate the basement membrane. Nonspecific staining is seen on the skin surface (white arrowheads). (**k**, **l**) By immunofluorescence staining, AKT activation (Ser-473 phosphorylated AKT; green) is observed in granular-layer keratinocytes of *Abca12*$^{-/-}$ mice. (**m**, **n**) Immunofluorescence staining for the Ki-67-proliferation marker shows similar staining patterns of basal keratinocytes in wild-type (**m**) and *Abca12*$^{-/-}$ (**n**) samples. (**a**, **b**, **e**, **f**; hematoxylin–eosin (H–E) stain. Bars of **c**, **d**, **g**, **h**, **i**, **j**, **k**, **l**, **m**, **n** = 20 μm. Bars of **a**, **b**, **e**, **f** = 5 μm.) (**o**) Immunoblot analysis shows that levels of serine-473-phosphorylated AKT (pAKT) in neonatal epidermis and differentiated keratinocytes of *Abca12*$^{-/-}$ mice are higher than those of wild-type mice.

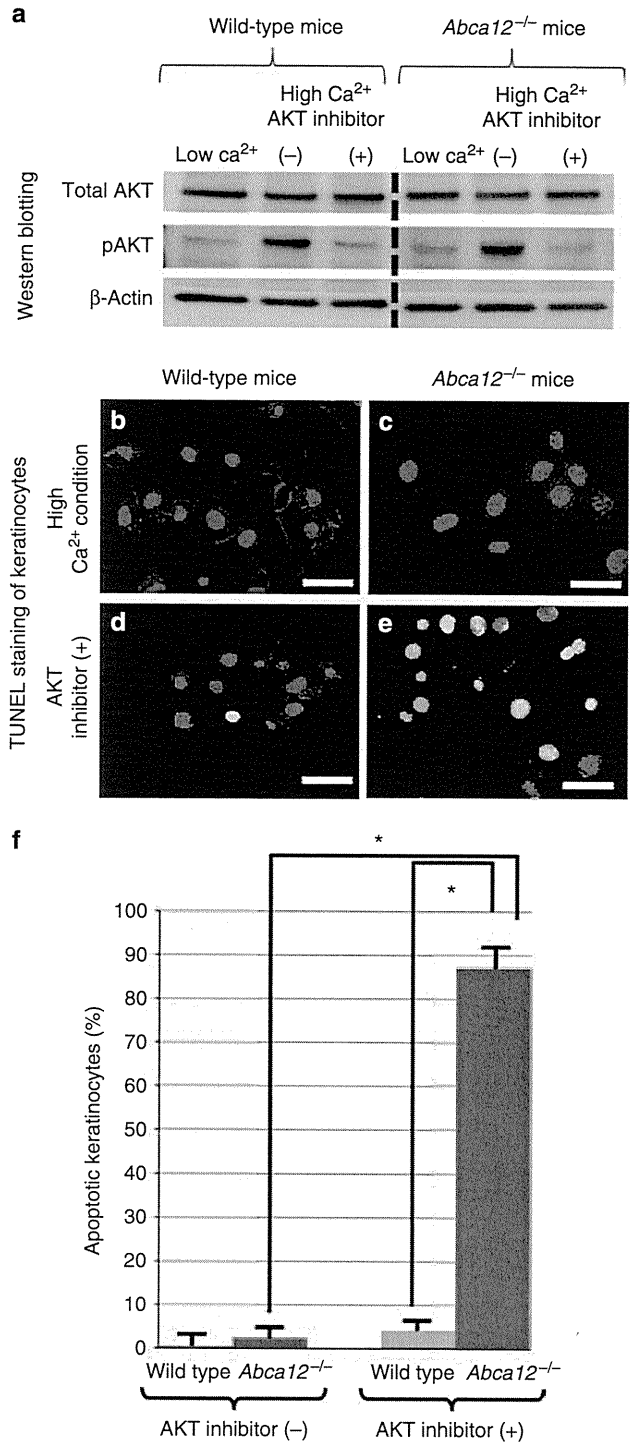

Figure 2. Inhibition of AKT activation leads to apoptosis of *Abca12*$^{-/-}$ keratinocytes. (**a**) Immunoblot analysis indicates that the AKT inhibitor can inhibit AKT activation (phosphorylated AKT (pAKT) synthesis) in differentiated keratinocytes. (**b**–**e**) TUNEL staining of keratinocytes cultured under high Ca^{2+} condition treated with/without the AKT inhibitor. Neither wild-type cells (**b**) nor *Abca12*$^{-/-}$ cells (**c**) are TUNEL positive. *Abca12*$^{-/-}$ keratinocytes with the AKT inhibitor (#124017; 10 μM) show many TUNEL-positive nuclei (**e**), although only a small number of wild-type cells with the AKT inhibitor are TUNEL positive (**d**). (Bars = 20 μm.) (**f**) Percentage of TUNEL-positive keratinocytes. *Abca12*$^{-/-}$ keratinocytes with AKT inhibitor shows a significantly greater number of TUNEL-positive nuclei than wild-type keratinocytes with/without the AKT inhibitor and *Abca12*$^{-/-}$ keratinocytes without the AKT inhibitor. ($n = 3$, mean ± SD, $^*P < 0.05$).

Although *Abca12*$^{-/-}$ granular-layer keratinocytes show characteristics of apoptosis, including condensed nuclei and positive TUNEL labeling, they are able to form epidermal stratification. In several disorders involving keratinocyte apoptosis, e.g., toxic epidermal necrolysis, the apoptotic epidermal keratinocytes show not only TUNEL-positive nuclei but also defective epidermal stratification (Abe *et al.*, 2003). Thrash *et al.* (2006) reported that AKT1 activation is an essential signal for keratinocyte cell survival and stratification, by experiments with gene silencing and three-dimensional cell cultures. Thus, we hypothesized that the AKT pathway might work as a compensatory mechanism against apoptosis in *Abca12*$^{-/-}$ keratinocytes. We have clearly shown that AKT activation occurs in *Abca12*$^{-/-}$ granular-layer keratinocytes, which suggests that AKT activation serves to prevent the cell death of *Abca12*$^{-/-}$ keratinocytes. By immunoblot analysis using anti-AKT1/2/3 antibodies (#2938/3063/3788, Cell Signaling), *Abca12*$^{-/-}$ epidermis showed expression of AKT1 and AKT2, but not AKT3 (Supplementary Figure S2 online). Compared with wild-type epidermis, *Abca12*$^{-/-}$ epidermis seemed to have more AKT1 than AKT2. From our data and the literature (Thrash *et al.*, 2006), we are able to speculate that AKT1 is the major isoform of phosphorylated AKT in *Abca12*$^{-/-}$ epidermis.

We have shown that PPAR-δ is a candidate molecule in the upstream of the AKT activation pathway in *Abca12*$^{-/-}$ keratinocytes. Di-Poi *et al.* (2002) reported that PPAR-δ has an anti-apoptotic role in keratinocytes via transcriptional control of the AKT1 signaling pathway. PPAR-δ also regulates the expression of ABCA12 (Jiang *et al.*, 2008). From these studies, we can speculate that upregulation of PPAR-δ is in response to apoptosis or decreased ABCA12 expression. To ascertain the function of PPAR-δ, we performed the experiments using a PPAR-δ-specific antagonist (GSK0660, Santa Cruz). Differentiated *Abca12*$^{-/-}$ keratinocytes treated with 1 μM GSK0660 for 48 hours showed TUNEL-positive nuclei, from which we are able to speculate an anti-apoptotic role for

PPAR-δ in *Abca12*$^{-/-}$ keratinocytes (Supplementary Figure S1 online). From our studies and the literature (Di-Poi *et al.*, 2002), PPAR-δ has been shown to have at least an anti-apoptotic role in *Abca12*$^{-/-}$ keratinocytes; however, it remains unclear whether the upregulation of PPAR-δ is in response to apoptosis or decreased ABCA12 expression.

Furthermore, we have measured the mRNA expression levels of other nuclear hormone receptors, including PPAR-α, PPAR-γ, retinoic acid receptor-α, liver X receptor-α, liver X receptor-β, RXR-α, and RXR-γ (Applied Biosystems). The mRNA level of RXR-α from *Abca12*$^{-/-}$ epidermis was shown to be significantly higher than that from wild-type epidermis (Supplementary Figure S1 online). The interaction between the upregulation of RXR-α and AKT activation in keratinocytes has not been reported. However, Wang *et al.* (2011) reported that RXR-α ablation in the epidermis enhances UV-induced apoptosis, which suggests that RXR-α has an anti-apoptotic function in keratinocytes. Thus, upregulation of RXR-α may also have an anti-apoptotic function in *Abca12*$^{-/-}$ keratinocytes.

In conclusion, the present data suggest that keratinocyte apoptosis is involved in the pathomechanisms of HI and that the AKT signaling pathway helps *Abca12*$^{-/-}$ keratinocytes to survive during the keratinization process. In light of this, activation of the AKT signal pathway may be to our knowledge, previously unreported strategy for treating keratinization disorders, including ichthyosis.

CONFLICT OF INTEREST

The authors state no conflict of interest.

ACKNOWLEDGMENTS

We thank Ms Aoyanagi for her technical assistance. This work was supported in part by a grant-in-aid from the Ministry of Education, Science, Sports and Culture of Japan (Kiban A 23249058: to MA), a grant from the Ministry of Health, Labor and Welfare of Japan (Health and Labor Sciences Research Grants; Research on Intractable Disease: H22-177: to MA), and a grant-in-aid from the Japan Society for the Promotion of Science Fellows (to TY).

***Teruki Yanagi*[1], *Masashi Akiyama*[1,2], *Hiroshi Nishihara*[3], *Yuki Miyamura*[1], *Kaori Sakai*[1], *Shinya Tanaka*[4] and *Hiroshi Shimizu*[1]**

[1]Department of Dermatology, Hokkaido University Graduate School of Medicine, Sapporo, Japan; [2]Department of Dermatology, Nagoya University Graduate School of Medicine, Nagoya, Japan; [3]Laboratory of Translational Pathology, Hokkaido University Graduate School of Medicine, Sapporo, Japan and [4]Laboratory of Cancer Research, Department of Pathology, Hokkaido University Graduate School of Medicine, Sapporo, Japan
E-mail: makiyama@med.nagoya-u.ac.jp

SUPPLEMENTARY MATERIAL

Supplementary material is linked to the online version of the paper at http://www.nature.com/jid

REFERENCES

Abe R, Shimizu T, Shibaki A *et al.* (2003) Toxic epidermal necrolysis and Stevens-Johnson syndrome are induced by soluble Fas ligand. *Am J Pathol* 162:1515–20

Akiyama M, Sugiyama-Nakagiri Y, Sakai K *et al.* (2005) Mutations in lipid transporter ABCA12 in harlequin ichthyosis and functional recovery by corrective gene transfer. *J Clin Invest* 115:1777–84

Di-Poi N, Tan NS, Michalik L *et al.* (2002) Antiapoptotic role of PPARbeta in keratinocytes via transcriptional control of the Akt1 signaling pathway. *Mol Cell* 10:721–33

Jiang YJ, Lu B, Kim P *et al.* (2008) PPAR and LXR activators regulate ABCA12 expression in human keratinocytes. *J Invest Dermatol* 128:104–9

Mitsutake S, Suzuki C, Akiyama M *et al.* (2010) ABCA12 dysfunction causes a disorder in glucosylceramide accumulation during keratinocyte differentiation. *J Dermatol Sci* 60:128–9

Moskowitz DG, Fowler AJ, Heyman MB *et al.* (2004) Pathophysiologic basis for growth failure in children with ichthyosis: an evaluation of cutaneous ultrastructure, epidermal permeability barrier function, and energy expenditure. *J Pediatr* 145:82–92

Sun P, Wang XQ, Lopatka K *et al.* (2002) Ganglioside loss promotes survival primarily by activating integrin-linked kinase/Akt without phosphoinositide 3-OH kinase signaling. *J Invest Dermatol* 119:107–17

Thrash BR, Menges CW, Pierce RH *et al.* (2006) AKT1 provides an essential survival signal required for differentiation and stratification of primary human keratinocytes. *J Biol Chem* 281:12155–62

Uchida Y, Houben E, Park K *et al.* (2010) Hydrolytic pathway protects against ceramide-induced apoptosis in keratinocytes exposed to UVB. *J Invest Dermatol* 130: 2472–80

Wang XQ, Sun P, Paller AS (2001) Inhibition of integrin-linked kinase/protein kinase B/Akt signaling: mechanism for ganglioside-induced apoptosis. *J Biol Chem* 276:44504–11

Wang Z, Coleman DJ, Bajaj G *et al.* (2011) RXRalpha ablation in epidermal keratinocytes enhances UVR-induced DNA damage, apoptosis, and proliferation of keratinocytes and melanocytes. *J Invest Dermatol* 131:177–87

Yanagi T, Akiyama M, Nishihara H *et al.* (2008) Harlequin ichthyosis model mouse reveals alveolar collapse and severe fetal skin barrier defects. *Hum Mol Genet* 17:3075–83

Yanagi T, Akiyama M, Nishihara H *et al.* (2010) Self-improvement of keratinocyte differentiation defects during skin maturation in ABCA12-deficient harlequin ichthyosis model mice. *Am J Pathol* 177:106–18

See related commentary on pg 1790

Interpretation of Skindex-29 Scores: Cutoffs for Mild, Moderate, and Severe Impairment of Health-Related Quality of Life

Journal of Investigative Dermatology (2011) **131,** 1945–1947; doi:10.1038/jid.2011.138; published online 19 May 2011

TO THE EDITOR

Health-related quality of life (HRQL) is commonly assessed by means of standardized questionnaires and expressed in domain and overall HRQL scores. An important challenge is to interpret these scores correctly. What does a given score really mean? Although there is no standard approach, several methods exist to facilitate the interpretation of HRQL scores.

In a recently published study (Prinsen *et al.*, 2010), we identified

Abbreviation: HRQL, health-related quality of life

[2] Gudbjartsson DF, Thorvaldsson T, Kong A, Gunnarsson G, Ingolfsdottir A. Allegro version 2. Nat Genet 2005;37:1015–6.
[3] Matise TC, Chen F, Chen W, De La Vega FM, Hansen M, He C, et al. A second-generation combined linkage physical map of the human genome. Genome Res 2007;17:1783–6.

Musharraf Jelani
Muhammad Tariq
Department of Biochemistry, Faculty of Biological Sciences, Quaid-i-Azam University, Islamabad, Pakistan

Iftikhar Ahmad Jan
Hazrat Ullah
Department of Pediatric Surgery, National Institute of Rehabilitation Medicine (NIRM), Islamabad, Pakistan

Muhammad Naeem
Department of Biotechnology, Faculty of Biological Sciences, Quaid-i-Azam University, Islamabad, Pakistan

Wasim Ahmad*
Department of Biochemistry, Faculty of Biological Sciences, Quaid-i-Azam University, Islamabad, Pakistan

*Corresponding author. Tel.: +92 51 90643003; fax: +92 51 9205753
E-mail address: ahmad115@hotmail.com wahmad@qau.edu.pk (W. Ahmad)

30 June 2010
doi:10.1016/j.jdermsci.2010.11.014

Letter to the Editor

New insight into genotype/phenotype correlations in *ABCA12* mutations in harlequin ichthyosis

Harlequin ichthyosis (HI) is a severe and often fatal congenital ichthyosis with an autosomal recessive inheritance pattern [1]. The clinical features include thick, plate-like scales with ectropion, eclabium and flattened ears. *ABCA12* mutations underlie HI [2,3] and it was clarified that HI is caused by severe functional defects in the keratinocyte lipid transporter ABCA12 [2]. To date, various *ABCA12* mutations have been reported in HI patients [4]. However, genotype/phenotype correlations in *ABCA12* mutations have been poorly elucidated. In order to obtain clues to understand genotype/phenotype correlations in *ABCA12* mutations, we report two HI patients from two independent Japanese families, who were compound heterozygotes for *ABCA12* mutations.

Patient 1 is the second child of healthy, unrelated Japanese parents. The skin of the baby girl was covered with white, diamond shaped plaques at birth (Fig. 1a). After therapy with oral retinoids and local application of white petrolatum, in a humid incubator, the scales gradually detached and passive and spontaneous mobility of the joints increased. Now at the age of 1 year and 7 months, her general condition is good, although she still has white to grey scales on a background of erythematous skin over her entire body. Patient 2 is the fourth child of healthy, unrelated Japanese parents. Her older brother had a history of congenital ichthyosis and died in early infancy. The skin of the newborn showed serious symptoms with thick, white, diamond shaped plaques, partly bordered by bleeding fissures (Fig. 1c). Although she had therapy with oral retinoids and local application of white petrolatum, in a humid incubator, her clinical symptoms failed to show any apparent improvement and she died when she was 5 months old.

Skin biopsies showed thick stratum corneum in both patients (Fig. 1d–g). In Patient 2, parakeratosis was observed in the epidermis and a sparse inflammatory cell infiltration was seen in the superficial dermis (Fig. 1e inset). Electron microscopy (Hitachi, Tokyo, Japan) revealed a large number of abnormal, variously sized lipid droplets that accumulated in the cornified cells of both patients' epidermis.

Mutational analysis of *ABCA12* was performed in both patients and their families. Each genomic DNA sample was subjected to PCR amplification, followed by direct automated sequencing. Oligonucleotide primers and PCR conditions used for amplification of all exons 1–53 of *ABCA12* were originally derived from the report by Lefèvre et al. [5] and were partially modified for the present study. The entire coding region including the exon/intron boundaries for both forward and reverse strands from the patients, their parents and 50 healthy Japanese controls were also sequenced. Both patients had the same paternal novel nonsense mutation p.Arg1515X (Fig. 1h) which leads to truncation of the first ATP-binding cassette within ABCA12 likely resulting in ABCA12 loss of function (Fig. 2a). On the other allele, Patient 1 had a maternal recurrent splice acceptor site mutation c.3295-2A>G (Fig. 1h). This splice site mutation was reported in an unrelated Japanese family with HI and was shown to lead to comparable amounts of 2 splice pattern variants [2]. The first mutant transcript would result in a 3 amino acids deletion (1099_1101delYMK). These 3 amino acids are located in the first transmembrane domain and are highly conserved (Fig. 2b). The second mutant transcript lost a 170-bp sequence from exon 24, which led to a frameshift. Expression of a small amount of ABCA12 protein, although mutated, was detected in the granular layer keratinocytes of the patient's epidermis and cultured keratinocytes by immunofluorescent staining [2]. Thus, it is possible that Patient 1 expresses some mutated ABCA12 protein with a partial function. This might be the reason why Patient 1 survived beyond the perinatal and neonatal period and is still alive although this might also be in part due to the prompt oral retinoid treatment.

Patient 2 carried a maternal missense mutation p.Gly1179Arg on the other locus (Fig. 1h). To confirm the presence of the mutation p.Gly1179Arg in Patient 2, we performed restriction enzyme digestion analysis using *BclI* (NEW ENGLAND BioLabs). Restriction enzyme digestion of PCR products was carried out according to the manufacture's protocols. The 255-bp PCR products from wild type alleles were not digested by *BclI*, although the PCR products from the allele with the mutation p.Gly1179Arg were digested into 173- and 82-bp fragments. The father's PCR product after *BclI* digestion showed a single 255-bp band, which indicated he had only normal alleles. In contrast, the PCR product after *BclI* digestion from the mother of Patient 2 showed 255-, 173- and 82-bp bands, which indicated that she was heterozygous for the p.Gly1179Arg missense mutation (supplementary Fig. S1). This mutation was reported in a

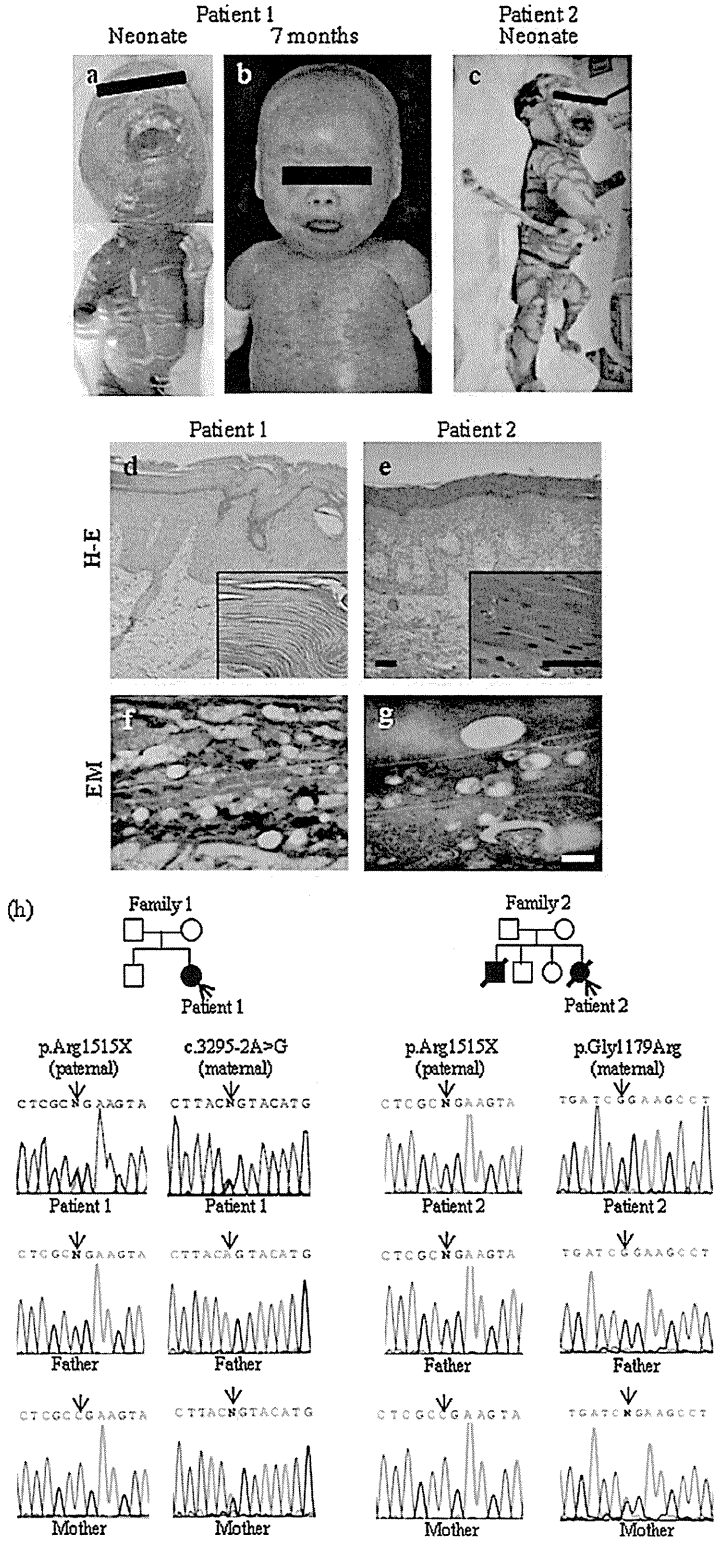

Fig. 1. (a–c) Clinical features of HI patients. Patient 1 showed the typical clinical phenotype of HI during the neonatal period, including the face and trunk (a). Her clinical symptoms remarkably improved at 7 months of age (b). Patient 2 showed more serious symptoms with thick plate-like scales and skin fissures in the neonatal period (c) and lived until the age of 5 months. (d–g) Histological features of the skin lesions of HI patients. Skin biopsies showed thick stratum corneum in both patients. Bars, 50 μm (d and e). In Patient 2, parakeratosis were observed (e, inset). By electron microscopy, abnormal variously sized lipid droplets had accumulated in the cornified cells of both patients' epidermis. Bars, 200 nm (f and g). (h) Families with HI and *ABCA12* mutations. Patient 1 was a compound heterozygote for two *ABCA12* mutations, a novel nonsense mutation p.Arg1515X and a recurrent splice site mutation c.3295-2A>G, and both her parents were heterozygous carriers. Patient 2 harboured two *ABCA12* mutations, p.Arg1515X and p.Gly1179Arg, and both her parents were heterozygous carriers of these defects.

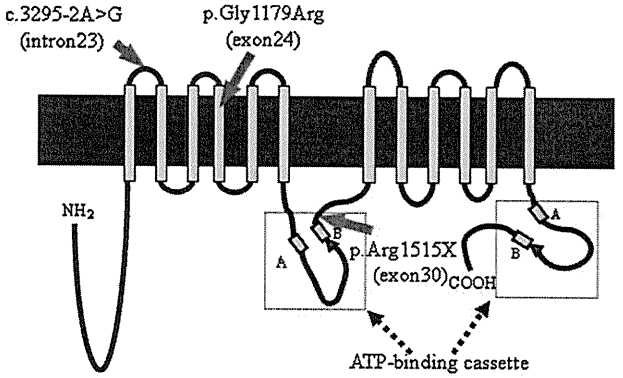

c.3295-2A>G: 1099_1101delYMK

Homo sapiens	1089 VYEKDLRLHEYMKMMGVNSCSHF 1111
Rattus norvegius	VYEKDLRLHEYMKMMGVNSCSHF
Mus musculus	VYEKDLRLHEYMKMMGVNSCSHF
Gallus gallus	VQEKDLRLYEYMKMMGVNASSHF
Danio rerio	VHERELRLHEYMKMMGVNPISHF

p.Gly1179Arg

Homo sapiens	1165 ISVFFNNTNIAALIGSLIYIIAFFPFIVL 1193
Rattus norvegius	ISVFFNNTNIAALIGSLIYVIAFFPFIVL
Mus musculus	ISVFFNNTNIAALIGSLIYVIAFFPFIVL
Gallus gallus	ISVFFNNTNIAALVGSLVYILTFFPFIVL
Danio rerio	VSSFFDKTNIAGLSGSLIYVISFFPFIVL

Fig. 2. (a) Structure of ABCA12 protein and the three mutations in present HI families. Dark blue area, cell membrane; bottom of dark-blue area, cytoplasmic surface. Note the mutation shared between the two patients is a truncation mutation in the first ATP-binding cassette (p.Arg1515X). The other mutation in Patient 2 is just a missense mutation in the first cluster of transmembrane domains (p.Gly1179Arg). (b) ABCA12 amino acid sequence alignment shows the level of conservation in diverse species of the amino acids, 1099_1101delYMK and p.Gly1179Arg (red characters).

Laotian family [6]. The glycine 1179 is a highly conserved amino acid residue (Fig. 2b) located in the first transmembrane ABCA12 domain (Fig. 2a), and this mutation substitutes an uncharged polar glycine residue for a positively charged arginine residue. The presence of these mutations was excluded in 100 alleles of 50 normal unrelated Japanese individuals.

Determinants of genotype/phenotype correlations resulting from *ABCA12* mutations, typically demonstrate that homozygotes or compound heterozygotes with truncation *ABCA12* mutations lead to an HI phenotype. Only a few exceptional cases have been reported such as the present case. The mutation p.Gly1179Arg might result in major loss of ABCA12 function and/or structure, leading to the severe phenotype in Patient 2.

Recently, long-term survival of patients with HI has been more frequently observed and documented [7,8]. The clinical symptoms of Patient 1 showed a remarkable improvement during infancy. In contrast, the symptoms of Patient 2 did not improve, and she died at the age of 5 months. The marked difference in the clinical severity of the two patients indicated that the p.Gly1179Arg has far bigger deleterious functional effects than c.3295-2A>G. The present study clearly demonstrates that some missense *ABCA12* mutations within highly conserved transmembrane regions are able to cause drastic changes in protein structure and function, leading to severe phenotypes, similar to truncation mutation patients. Further accumulation of similar cases is needed to confirm genotype/phenotype correlation in *ABCA12* mutations, especially in studies involving missense mutations underlying HI.

Acknowledgments

We thank Dr. James R. McMillan for proofreading the manuscript. This work was supported in part by a grant-in-aid from the Ministry of Education, Science, Sports and Culture of Japan (Kiban B 20390304: to M.A.), a grant from Ministry of Health, Labour and Welfare of Japan (Health and Labour Sciences Research Grants; Research on Intractable Disease: H22-177: to M.A.).

Appendix A. Supplementary data

Supplementary data associated with this article can be found, in the online version, at doi:10.1016/j.jdermsci.2010.11.010.

References

[1] Akiyama M. Harlequin ichthyosis and other autosomal recessive congenital ichthyoses: the underlying genetic defects and pathomechanisms. J Dermatol Sci 2006;42:83–9.
[2] Akiyama M, Sugiyama-Nakagiri Y, Sakai K, McMillan JR, Goto M, Arita K, et al. Mutations in ABCA12 in harlequin ichthyosis and functional rescue by corrective gene transfer. J Clin Invest 2005;115:1777–84.
[3] Kelsell DP, Norgett EE, Unsworth H, Teh MT, Cullup T, Mein CA, et al. Mutations in ABCA12 underlie the severe congenital skin disease harlequin ichthyosis. Am J Hum Genet 2005;76:794–803.
[4] Akiyama M. ABCA12 mutations and autosomal recessive congenital ichthyosis: a review of genotype/phenotype correlations and of pathogenetic concepts. Hum Mutat 2010;31(July):1090–6.
[5] Lefèvre C, Audebert S, Jobard F, Bouadjar B, Lakhdar H, Boughdene-Stambouli O, et al. Mutations in the transporter ABCA12 are associated with lamellar ichthyosis type 2. Hum Mol Genet 2003;12:2369–78.
[6] Thomes AC, Cullup T, Norgett EE, Hill T, Barton S, Dale BA, et al. ABCA12 is the major harlequin ichthyosis gene. J Invest Dermatol 2006;126:2408–13.
[7] Akiyama M, Sakai K, Sato T, McMillan JR, Goto M, Sawamura D, et al. Compound heterozygous ABCA12 mutations including a novel nonsense mutation underlie harlequin ichthyosis. Dermatology 2007;215:155–9.
[8] Akiyama M, Sakai K, Wolff G, Hausser I, McMillan JR, Sawamura D, et al. A novel ABCA12 mutation 327delT causes harlequin ichthyosis. Br J Dermatol 2006;155:1064–6.

H. Umemoto[a,b]
[a]*Department of Dermatology, Hokkaido University Graduate School of Medicine, Sapporo, Japan*
[b]*Department of Oral Diagnosis and Oral Medicine, Hokkaido University Graduate School of Dental Medicine, Sapporo, Japan*

M. Akiyama[a,b,*]
[a]*Department of Dermatology, Hokkaido University Graduate School of Medicine, Sapporo, Japan*
[b]*Department of Dermatology, Nagoya University Graduate School of Medicine, Nagoya, Japan*

T. Yanagi
K. Sakai
Department of Dermatology, Hokkaido University Graduate School of Medicine, Sapporo, Japan

Y. Aoyama
Department of Dermatology, Okayama University Graduate School of Medicine, Okayama, Japan

A. Oizumi
Y. Suga
Department of Dermatology, Juntendo University School of Medicine, Urayasu Hospital, Urayasu, Japan

Cell Stem Cell
Article

Hair Follicle Stem Cells Provide a Functional Niche for Melanocyte Stem Cells

Shintaro Tanimura,[1,2,9] Yuko Tadokoro,[1,9] Ken Inomata,[1,3] Nguyen Thanh Binh,[1,8] Wataru Nishie,[2] Satoshi Yamazaki,[4,5] Hiromitsu Nakauchi,[4,5] Yoshio Tanaka,[1] James R. McMillan,[2] Daisuke Sawamura,[6] Kim Yancey,[7] Hiroshi Shimizu,[2] and Emi K. Nishimura[1,2,8,*]

[1]Department of Stem Cell Medicine, Cancer Research Institute, Kanazawa University, Kanazawa, Ishikawa 920-0934, Japan
[2]Department of Dermatology, Hokkaido University Graduate School of Medicine, Sapporo 060-8638, Japan
[3]Fundamental Research Laboratories, KOSÉ Corporation, 1-18-4 Azusawa, Itabashi-ku, Tokyo 174-0051, Japan
[4]Japan Science and Technology Agency (JST), ERATO, Sanbacho, Chiyoda-ku, Tokyo 102-0075, Japan
[5]Division of Stem Cell Therapy, Center for Stem Cell Biology and Regenerative Medicine, The Institute of Medical Science, The University of Tokyo, 4-6-1 Shirokanedai, Minato-ku, Tokyo 108-8639, Japan
[6]Department of Dermatology, Hirosaki University, School of Medicine, Hirosaki, Aomori 036-8562, Japan
[7]Department of Dermatology, University of Texas Southwestern Medical Center in Dallas, Dallas, TX 75390-9069, USA
[8]Department of Stem Cell Biology, Medical Research Institute, Tokyo Medical and Dental University, 2-3-10 Kanda Surugadai, Chiyoda-ku, Tokyo 101-0062, Japan
[9]These authors contributed equally to this work
*Correspondence: nishscm@tmd.ac.jp
DOI 10.1016/j.stem.2010.11.029

SUMMARY

In most stem cell systems, the organization of the stem cell niche and the anchoring matrix required for stem cell maintenance are largely unknown. We report here that collagen XVII (COL17A1/BP180/BPAG2), a hemidesmosomal transmembrane collagen, is highly expressed in hair follicle stem cells (HFSCs) and is required for the maintenance not only of HFSCs but also of melanocyte stem cells (MSCs), which do not express *Col17a1* but directly adhere to HFSCs. Mice lacking *Col17a1* show premature hair graying and hair loss. Analysis of *Col17a1*-null mice revealed that COL17A1 is critical for the self-renewal of HFSCs through maintaining their quiescence and immaturity, potentially explaining the mechanism underlying hair loss in human *COL17A1* deficiency. Moreover, forced expression of *COL17A1* in basal keratinocytes, including HFSCs, in *Col17a1*-null mice rescues MSCs from premature differentiation and restores TGF-β signaling, demonstrating that HFSCs function as a critical regulatory component of the MSC niche.

INTRODUCTION

The stem cell microenvironment, or niche, is critical for stem cell maintenance (Li and Xie, 2005; Moore and Lemischka, 2006). Accumulating evidence has confirmed that cell-cell and cell-extracellular matrix adhesion within the niche is essential for the establishment and maintenance of niche architecture in different stem cell systems (Raymond et al., 2009). Adhesion to the underlying extracellular matrix has been suggested as an important factor in epidermal stem cell maintenance (Green, 1977; Watt, 2002), but a specific stem-cell anchoring matrix for stem cell maintenance has not yet been identified. Hair follicle stem cells (HFSCs) are found in the hair follicle bulge, a distinct area of the outer root sheath that overlies the basement membrane at the lower permanent portion in mammalian hair follicles (Blanpain and Fuchs, 2006; Cotsarelis, 2006). The HFSC population is composed of multipotent keratinocyte stem cells and is responsible for the cyclic regeneration of hair follicles as well as a transient supply of progeny to the interfollicular epidermis (IFE) and to sebaceous glands after wounding (Blanpain and Fuchs, 2006; Cotsarelis, 2006; Oshima et al., 2001). The HFSC population in the bulge area normally supplies a short-term reservoir to the secondary hair germ (subbulge area), which is located just below the bulge area but above the dermal papilla and corresponds to the lowermost portion of resting hair follicles (Figure S1A available online; Greco et al., 2009). Melanocyte stem cells (MSCs), which are originally derived from the neural crest, also reside in the follicular bulge-subbulge area (Figure S1A). MSCs supply pigment-producing melanocytes to the hair matrix during each hair cycle to maintain hair pigmentation (Nishimura et al., 2002). Therefore, the bulge-subbulge area houses at least two distinct stem cell populations with different origins. However, it is still unclear to what extent these two different stem cells interact to promote each other's maintenance.

Hemidesmosomes are multiprotein adhesion complexes that promote stable epidermal-dermal attachments. The transmembrane protein collagen XVII (COL17A1/BP180/BPAG2) is a structural component of the outer hemidesmosomal plaque, which projects beneath hemidesmosomes in epidermal basal keratinocytes into the underlying basement membrane to mediate anchorage (Masunaga et al., 1997; Nishizawa et al., 1993; Powell et al., 2005). In patients with *COL17A1* deficiency, a subtype of congenital junctional epidermolysis bullosa blistering disease, hemidesmosomes are poorly formed (McGrath et al., 1995; Nishie et al., 2007) and there is a characteristic premature hair loss (alopecia) with hair follicle atrophy (Darling et al.,

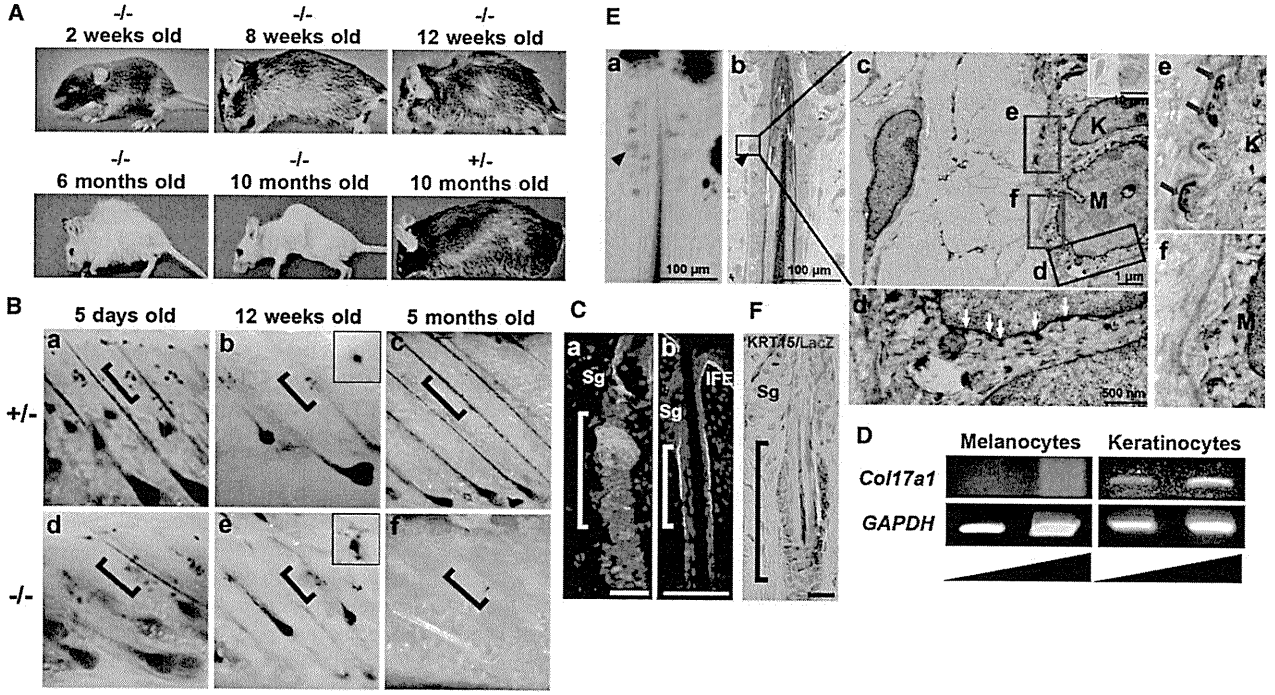

Figure 1. Hair Graying and Hair Loss Are Preceded by Depletion of MSCs in *Col17a1* Deficiency

(A) Macroscopic phenotype of *Col17a1*$^{-/-}$ mice at different times as noted and of *Col17a1*$^{+/-}$ littermates at 10 months of age.

(B) Deletion of *Col17a1* affects the maintenance of MSCs in the bulge-subbulge area. The distribution and morphology of *Dct-lacZ*-expressing melanoblasts is normal in the bulge-subbulge area of 5-day-old *Col17a1*$^{-/-}$ mice (a and d). At 12 weeks of age, abnormal melanocytes with dendritic morphology were found in the bulge area of *Col17a1*$^{-/-}$ anagen follicles (e). Inset in (e) shows magnified view of ectopically pigmented melanocytes in the hair follicle bulge-subbulge of *Col17a1*$^{-/-}$ mice. By 5 months of age, *Dct-lacZ*-expressing cells were lost both in the bulge-subbulge area and in the hair bulb (f). Bulge-subbulge areas are demarcated by brackets.

(C) COL17A1 expression in the bulge area (demarcated by brackets). (a) COL17A1 (a: red) is expressed in KRT15 (a: green)-expressing bulge keratinocytes and in basal cells of the IFE (b: green) in wild-type skin. (b) *Dct-lacZ*-expressing melanoblasts (b: red) are located close to COL17A1^{+} basal cells (b: green) in wild-type follicles. Scale bars represent 40 μm.

(D) RT-PCR analysis; the level of *Col17a1* mRNA is below the detection limit in flow cytometry-sorted GFP-tagged melanoblasts.

(E) Light and electron micrographs of *Dct-lacZ*-expressing melanoblasts in the bulge area (MSCs). The arrowheads in (a) and (b) point to *Dct-lacZ*-expressing melanocytes in the bulge areas in semithin sections of the skin. The ultrastructural high-power view is of the boxed areas shown in (b) and (c). X-gal reaction products accumulated in association with the nuclear membrane (d: white arrows). *Dct-lacZ*-expressing melanocytes lack hemidesmosome formation in the basement membrane zone (f), whereas adjacent keratinocytes form mature hemidesmosomes in the bulge area (e: red arrows).

(F) *Dct-lacZ*-expressing melanoblasts (blue) are in direct contact with keratin 15 (KRT15)-expressing keratinocytes in the bulge area (yellow brown). Scale bar represents 20 μm.

M, melanocytes in bulge; K, keratinocytes in bulge; Sg, sebaceous gland; IFE, interfollicular epidermis. See also Figure S1.

1997; Hintner and Wolff, 1982) that suggests that COL17A1 plays a role in hair follicle homeostasis. We previously reported premature hair loss in *Col17a1*-deficient mice (Nishie et al., 2007), although the precise underlying mechanism is unknown. In this study, we used *Col17a1* knockout mice and *COL17A1*-expressing transgenic mice to show that *Col17a1* plays essential roles in the maintenance of HFSCs, which provide a functional niche for MSCs.

RESULTS

Defective MSC Maintenance and Resultant Hair Graying in *Col17a1*-Null Mice

To understand the role of collagen XVII in hair follicle homeostasis, we performed a careful chronological analysis of *Col17a1*-deficient mice. As shown in Figure 1A, *Col17a1* null mice showed premature hair loss generally preceded by extensive hair graying. Conversely, heterozygous mice displayed a normal phenotype. The hair coats in *Col17a1*-null mice were indistinguishable from control littermates for 8 weeks after birth. However, progressive hair graying started from the snout at around 12 weeks of age and then became pronounced on their backs at around 4–6 months of age and was associated with a sparser hair distribution that was subsequently followed by progressive and more extensive hair loss (Figure 1A). It is notable that these hair changes were not accompanied or preceded by any apparent changes in the skin. Skin friction, such as attempting to artificially peel neonatal skin, can induce skin erosions in *Col17a1*-null mice (Nishie et al., 2007) but did not significantly accelerate hair graying or hair loss. Thus, it is unlikely that the hair changes are a secondary outcome of skin detachment but is more likely that the hair graying and hair loss are programmed through the

Col17a1 deficiency in the hair follicles. Our previous studies demonstrated that defective maintenance of MSCs in the hair bulge causes hair graying (Nishimura et al., 2005). Thus, we first examined the distribution and morphology of MSCs in *Col17a1*-null mice by using a melanocyte-targeted *Dct-lacZ* transgene (Mackenzie et al., 1997). As shown in Figures 1Ba and 1Bd, *Dct-lacZ*-expressing cells showed a normal morphology and distribution in the bulge area during hair follicle morphogenesis until initiation of the hair regeneration cycle both in *Col17a1*$^{+/-}$ and in *Col17a1*$^{-/-}$ mice. At around 12 weeks after birth, pigmented melanocytes with a dendritic morphology that expressed melanocyte markers appeared in the hair follicle bulge of *Col17a1*$^{-/-}$ mice (Figure 1Be; Figure S1Be). At 5 months of age, *Dct-lacZ*-expressing cells were almost completely lost in the follicle bulge area as well as in the hair bulbs of *Col17a1*-null mice (Figure 1Bf; Figure S1Bf). These data demonstrate that MSC maintenance is defective in *Col17a1*-deficient mice and that this mechanism results in progressive hair graying.

Preferential Expression of COL17A1 in HFSCs but Not in MSCs

Collagen XVII is a hemidesmosomal transmembrane collagen expressed by basal keratinocytes of the IFE (McGrath et al., 1995). However, neither the expression of mouse *Col17a1* nor hemidesmosome assembly in melanocyte lineage cells and/or in bulge keratinocytes has been reported, so we first examined the expression of mouse COL17A1 protein in hair follicles by using immunohistochemistry. As shown in Figure 1Ca and Figures S1C and S1D, mouse COL17A1 was preferentially localized along the dermal-epidermal junction of bulge keratinocytes that express markers for HFSCs but not in follicular keratinocytes outside of the bulge area. However, the localization of COL17A1 in basal cell surface of MSCs could not be determined via normal immunohistochemical methods, because the attachment site of MSCs to the basement membrane is limited (Figure 1Cb). We therefore examined *Col17a1* expression by using RT-PCR in flow cytometry-sorted GFP^{+} cells from melanocyte lineage-tagged GFP transgenic mouse skin (Osawa et al., 2005). In sharp contrast to the significant expression of *Col17a1* in control keratinocytes, expression in GFP^{+} melanocytes was not detectable (Figure 1D). To support this finding, we used transmission electron microscopy (TEM) to check whether *Dct-lacZ*-expressing melanoblasts within the bulge area in wild-type animals have hemidesmosomes. As shown in Figure 1E, hemidesmosomes, which form regularly spaced electron-dense structures along the epidermal basement membrane zone (McMillan et al., 2003), were completely absent in *Dct-lacZ*-expressing melanoblasts in the bulge (Figures 1Ed and 1Ef), whereas typical hemidesmosomes were seen overlying the basal plasma membrane in surrounding bulge keratinocytes (Figure 1Ee). Because these bulge keratinocytes adjacent to *Dct-lacZ*-expressing melanoblasts express HFSC markers (Figure 1F), these data indicate that HFSCs but not MSCs are anchored to the underlying basement membrane via hemidesmosomes. We also confirmed the localization of COL17A1 to hemidesmosomes in basal keratinocytes but not in melanocytes by immunogold electron microscopic analysis of human epidermis (Figure S1E). Therefore, we conclude that MSCs do not express COL17A1 and do not assemble any discernible hemidesmosomal structures at their surface. These findings suggested that the depletion of MSCs in *Col17a1*-null mice is caused by defects in the HFSC population that forms the main supportive cells surrounding MSCs.

Abrogated Quiescence and Immaturity of HFSCs Result in Depletion of HFSCs in *Col17a1*-Null Mice

Previous studies on wild-type mouse skin reported that mature hemidesmosomes exist at the follicular-dermal junction just below the level of sebaceous glands (Hojiro, 1972) and in hair germs of telogen hair follicles (Greco et al., 2009). Consistently, we found mature hemidesmosomes at these junctions within the hair follicle bulge (Figure 1Ee). However, mature hemidesmosomes have not been found in the transient portion of hair follicles (Hojiro, 1972), where COL17A1 expression is undetectable. These data suggested that hemidesmosome formation is important for anchoring of HFSCs located in the bulge-subbulge area of hair follicles to the basal lamina.

To test whether the abnormalities observed in *Col17a1* deficiency are specifically caused by any functional defects of HFSCs or by their detachment from the basal lamina, we first carefully examined the junctions of hair follicles in the dorsal skin of *Col17a1*-null mice and their controls by TEM. A significant number of hemidesmosomes are poorly formed in the bulge keratinocytes of *Col17a1*-deficient mice (Figure S2B), as seen in epidermal keratinocytes of those mice (Nishie et al., 2007). However, we did not find any significant microscopic separation at the follicular-dermal junction in sections of trunk skin from *Col17a1*-null mice (Figure 2; Figures S2A and S2B). Furthermore, we did not find significant inflammatory cell infiltrates or any signs of cell death, such as the appearance of eosinophilic cell bodies or TUNEL-positive or cleaved caspase 3-positive cells, at the follicular-dermal junction area of *Col17a1*-null mouse skin (Figure S2C and data not shown). Basement membrane thickening/reduplication, a sign of repeated regeneration of the epidermal and dermal junction, was also not found. These findings suggested that the hair graying and hair loss phenotypes in *Col17a1*-null mice cannot be explained simply by HFSC detachment from the basal lamina but instead may result from dysregulation or altered cell properties of HFSCs caused by *Col17a1* deficiency.

To examine whether HFSCs show any dysregulation caused by *Col17a1* deficiency, we carefully examined the hair follicle cycle progression, which alternates phases of growth (anagen), regression (catagen), and rest (telogen) in synchronization with the activation status of HFSCs, in *Col17a1*-null mice. While the first short telogen phase was transiently seen around 22 days after birth both in *Col17a1*-null mice and in control littermates, the second telogen phase was significantly shortened in *Col17a1*-null mice (Figure 2, summarized on the right side). At 6 weeks of age, just before normal hair follicles on the dorsal skin enter the second telogen phase, most hair follicles in *Col17a1*$^{-/-}$ mice were not distinguishable from those in *Col17a1*$^{+/-}$ mice either in morphology or in hair cycle progression. The second telogen phase is normally seen at around 7 weeks after birth and lasts about 4–5 weeks over the entire skin surface of wild-type mice (Paus and Cotsarelis, 1999; Paus et al., 1999). This phase was shortened to less than 2 weeks in all *Col17a1*$^{-/-}$ mice examined at 8–12 weeks of age, whereas such an aberrant pattern was seen in only 14.3% of *Col17a1*$^{+/-}$ mice. The subsequent

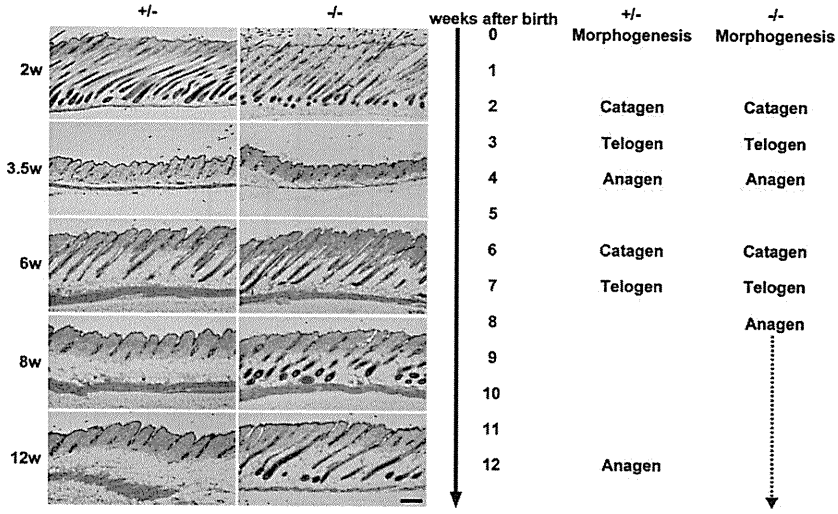

Figure 2. Loss or Shortening of the Resting State of Hair Follicles in *Col17a1*-Deficient Skin

Representative H&E images of dorsal skin sections (left) and time-scale for the hair cycle (right) from *Col17a1*$^{-/-}$ mice and from *Col17a1*$^{+/-}$ littermates during the first 12 weeks after birth. In *Col17a1*$^{-/-}$ follicles, the second telogen was significantly shortened, and the second anagen lasted longer. Scale bar represents 200 μm. See also Figure S2.

anagen phase was rather prolonged in *Col17a1*$^{-/-}$ mice compared to their control littermates. These findings suggest that HFSCs are unable to remain quiescent for a sufficient time from the second telogen phase and thereafter in the absence of *Col17a1*.

To search for early events or changes in HFSCs in *Col17a1*-null mice, we performed immunohistochemical analysis with four different markers for HFSCs, keratin 15 (KRT15), CD34, α6-integrin, and S100A6, at different stages (Figure 3A; Figure S3; Morris et al., 2004; Tumbar et al., 2004). At 5 weeks of age, there was no difference in the expression of HFSC markers or the number of HFSC marker-positive cells between control and *Col17a1*-null mice. However, at around 8 weeks of age, HFSC marker-expressing cells were absent in the bulge area in selected null mouse hair follicles (Figures 3A and 3B; Figure S3A), and the number of these marker-deficient follicles increased over time. By 6 months of age, the HFSC population had been lost in most hair follicles of *Col17a1*-null mice (Figure S3B). Flow cytometric analysis also confirmed that the α6-integrin^{high} CD34^{+} population (Blanpain and Fuchs, 2006), which represents basal HFSCs in the bulge area, was diminished (Figure 3C). Hair follicle atrophy with the loss of hair follicle structures were also observed once the HFSC population was diminished (Figure 3D). These data indicate that *Col17a1*-null HFSCs fail to maintain their stem cell characteristics, including their quiescence and immaturity, after the second telogen phase, resulting in hair follicle atrophy. Conversely, epidermal hyperplasia was also transiently found in some focal areas of the *Col17a1*-null skin at around 6 months of age (Figure 3D, arrowheads) but was normalized and subsequently became atrophic at later stages, which suggests that the epidermal stem cell population might also be gradually losing its self-renewing potential with age in *Col17a1* deficiency compared to controls.

To examine whether HFSC maintenance fails because the cells lose their immaturity or quiescence in the absence of *Col17a1*, we analyzed the expression of markers for keratinocyte differentiation and proliferation in *Col17a1*-null hair follicles. Interestingly, keratin 1 (KRT1), a differentiation marker for the IFE, was ectopically expressed in the bulge area of *Col17a1*-null mice at 8 weeks of age (Figure 4A). KRT1-positive cells in the bulge areas of affected hair follicles were found in 60% of *Col17a1*-null mice but not in control mice at that age. Ectopic expression of other epidermal differentiation markers, such as involucrin and KRT10, was also present in the bulge areas of *Col17a1*-null mice at 8 weeks of age (Figure S4A). Furthermore, Ki67-positive cells were located in the bulge area of *Col17a1*-null mice, and those Ki67-positive cells showed an absent or reduced level of KRT15 expression (Figure 4A).

The maintenance of quiescence and immaturity of somatic stem cells in tissues is a prerequisite for sustained stem cell self-renewal, and which can be assessed for HFSCs by means of a colony-formation assay in vitro (Barrandon and Green, 1987; Oshima et al., 2001). We therefore took advantage of the type of assay by using neonatal epidermal keratinocytes, which contain the presumptive HFSC population (Nowak et al., 2008), to assess the self-renewal potential of that population in *Col17a1*-null mice. As shown in Figures 4Ba and 4Bb, *Col17a1* homozygous null keratinocytes showed defects in colony-forming ability on 3T3-J2 feeder cells compared to keratinocytes from control mice. Colonies larger than 0.5 mm in diameter were significantly decreased in number with *Col17a1*-null keratinocytes (Figure 4Bc). Although *Col17a1*-null keratinocytes showed defective binding ability to collagen I-coated dishes (Figure S4B), they showed no detectable defects in their ability to directly adhere to 3T3-J2 feeder cells (Figure 4Bd). These data strongly suggest that *Col17a1*-null keratinocytes have a much lower renewal capability than control keratinocytes. Taken together with the in vivo findings, we conclude that COL17A1 is critical for the self-renewal of HFSCs by maintaining their immaturity and quiescence.

Loss of TGF-β Expression by HFSCs and the Associated Differentiation of Adjacent MSCs

To examine whether the early changes in HFSC in *Col17a1* mutant mice affects the maintenance of MSCs in the hair follicle bulge, we carefully examined MSCs in hair follicle bulge areas in *Col17a1*-null mice beginning to show HFSC defects. At 8 weeks of age, when HFSCs in *Col17a1*-null mice are prematurely activated, KIT^{+} melanoblasts within the bulge area prematurely coexpressed TYRP1, a melanocyte differentiation marker, in *Col17a1*-null mice but not in control mice (Figure S5A). At around 12 weeks of age, pigmented melanocytes with a mature

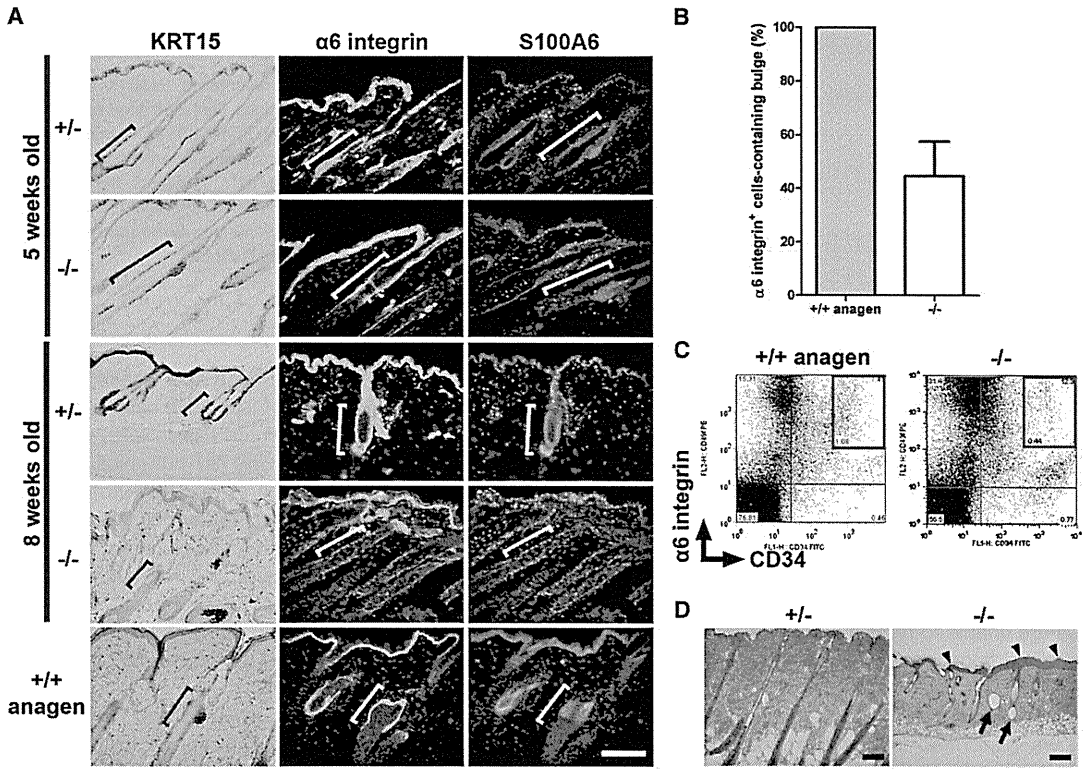

Figure 3. HFSC Depletion in COL17A1-Deficient Mice

(A) Immunostaining of the dorsal skin from *Col17a1*$^{-/-}$ and from *Col17a1*$^{+/-}$ mice with HFSC markers. The bulge areas are demarcated by brackets. HFSC marker (KRT15, α6-integrin, and S100A6)-expressing cells were still maintained at 5 weeks of age in *Col17a1*$^{-/-}$ mice, whereas follicles without HFSC marker-positive cells appeared at 8 weeks of age.

(B) Ratio of hair follicles with α6-integrin^{+} cells in the bulge areas of skin from control mice and from 8- to 10-week-old *Col17a1*$^{-/-}$ mice. In *Col17a1*$^{-/-}$ mice, many hair follicles without α6-integrin^{+} cells in the bulge areas were found (n = 3).

(C) Flow cytometric analysis of α6-integrin and CD34 double-labeled keratinocytes. α6-integrin^{+} CD34^{+} cells are almost completely lost in the skin of 9-month-old *Col17a1*$^{-/-}$ mice.

(D) H&E-stained histological sections of *Col17a1*$^{-/-}$ and of *Col17a1*$^{+/-}$ mouse skin. At 6 months of age, there was a diminution of hair follicle bulbs, degeneration of the hair follicles (arrows), and epidermal hyperplasia (arrowheads) in *Col17a1*$^{-/-}$ skin. As a control for the anagen phase in (A), (B), and (C), dorsal skin at 5 days after hair-plucking of telogen follicles was used.

Scale bars represent 100 μm. See also Figure S3.

dendritic morphology and expressing TYRP1 in addition to *Dct-lacZ* and KIT were aberrantly found within the bulge area in mid-anagen hair follicles (*Dct-lacZ*-expressing cells in Figure 1B, Figure S1B, arrow in Figure 5A; KIT^{+}/TYRP1^{+} cells in Figures 5B and 5C and Figure S5B). Conversely, only nonpigmented melanoblasts expressing *Dct-lacZ* and KIT but not TYRP1 and with small cell bodies (MSCs) were found in control littermates (Figure 1B; Figures S1B and S5B). Similar morphological changes were previously described as ectopic MSC differentiation within the niche (Inomata et al., 2009; Nishimura et al., 2005). These ectopically differentiated melanocytes were found in the bulge area at 12–13 weeks of age, prior to the hair graying seen in *Col17a1*-null mice (Figure 5D). Furthermore, it is notable that the ectopically differentiated melanocytes in *Col17a1*-deficient mice were typically found in association with early changes in bulge keratinocytes including the enlarged morphology of surrounding bulge keratinocytes (Figure 5A, arrowheads) and an increased number of Ki67-expressing bulge keratinocytes in midanagen follicles (Figures 4A and 5E and data not shown). The appearance of ectopically differentiated melanocytes within the bulge area was followed by progressive hair graying in *Col17a1*-null mice (Figures 1A and 1B; Figure S1B).

TGF-β signaling is activated in the hair follicle bulge and is involved in but is not essential for the maintenance of HFSCs (Guasch et al., 2007; Qiao et al., 2006; Yang et al., 2005, 2009). Our recent study showed that the signal is required for the maintenance of MSCs through promoting MSC immaturity and quiescence (Nishimura et al., 2010), but it was not clear whether the signal is derived from HFSCs or MSCs. As similar changes in MSCs, such as the appearance of ectopically differentiated melanocytes in the niche and the subsequent depletion of MSCs seen in *Col17a1*-null mice, were found in *TGFbRII* conditional knockout mice (Nishimura et al., 2010), we hypothesized that the defective renewal of MSCs in *Col17a1*-null mice might be mediated by defective TGF-β signaling from the surrounding HFSCs. To test this model, we examined the involvement of TGF-β signaling in the defects of MSCs in *Col17a1*-null mice and their controls. We found that KRT15-expressing

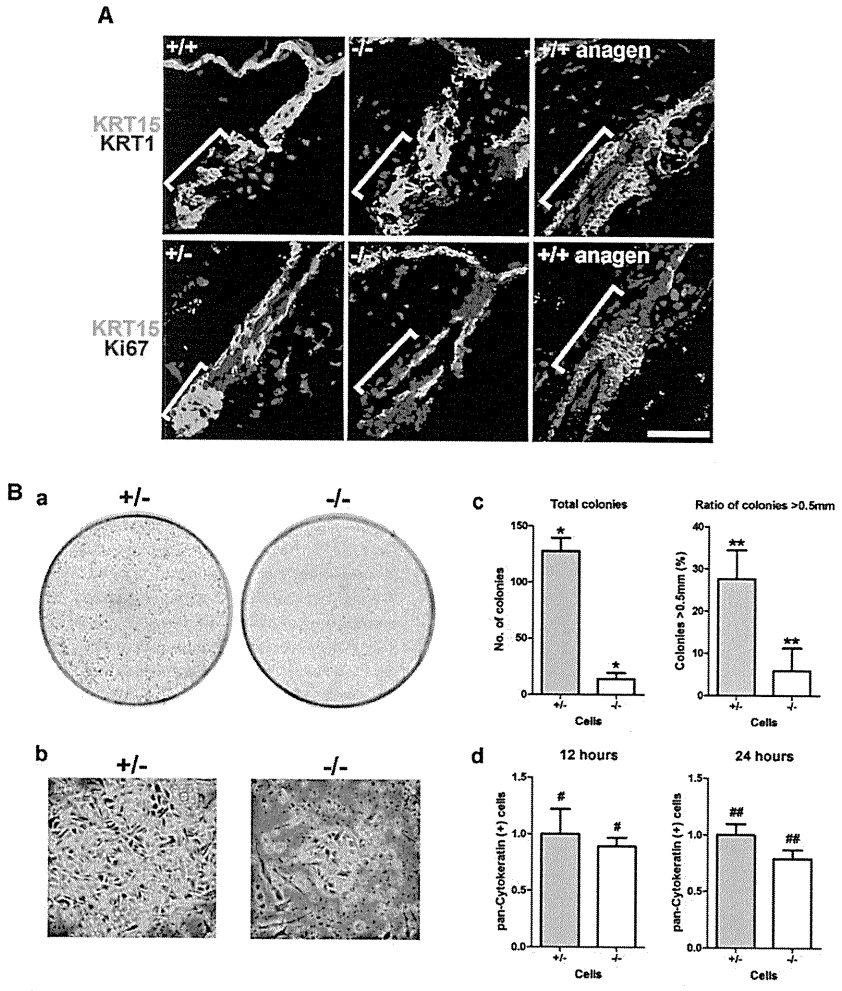

Figure 4. Deficient Stemness of HFSCs in *Col17a1*-Null Skin

(A) Immunostaining of the dorsal skin from 8-week-old *Col17a1*$^{-/-}$ and from control mice with the IFE differentiation marker keratin 1 (KRT1) and Ki67. The bulge areas are demarcated by brackets. Top: In *Col17a1*$^{-/-}$ mice, cells coexpressing KRT15 (green) and KRT1 (red) appeared within the bulge area. Bottom: Cells in the bulge area of *Col17a1*$^{-/-}$ mice proliferated abnormally. As a control for anagen phase, dorsal skin at 5 days after hair-plucking of telogen follicles was used. Scale bar represents 50 μm.

(B) Loss of keratinocyte clonal growth potential resulting from *Col17a1* deficiency. (a) Clonal growth assays of keratinocytes from *Col17a1*$^{-/-}$ and from *Col17a1*$^{+/-}$ mice; representative dishes are shown. (b) *Col17a1*$^{-/-}$ keratinocytes formed only small colonies. (c) Colonies from *Col17a1*$^{-/-}$ skin were significantly fewer and smaller than those from *Col17a1*$^{+/-}$ control mice. *, **$p < 0.05$. (d) Keratinocytes from *Col17a1*$^{-/-}$ skin did not show decreased binding to 3T3-J2 feeder cells. $^{\#}p = 0.6653$, $^{\#\#}p = 0.162$.

See also Figure S4.

keratinocytes coexpress TGF-β1/2 in wild-type hair follicles (Figure 5F), demonstrating that HFSCs produce TGF-β1/2 in the bulge area. At 6 weeks of age, the expression of TGF-β1/2 was similar in bulge keratinocytes in the control and in *Col17a1*-null mice (Figure 5G). At 8 weeks of age or later, however, the hair follicle bulge exhibited significantly downregulated expression of TGF-β1/2 in *Col17a1*-null mice, although the hair follicle bulge in control mice showed a normal expression pattern (Figure 5G). Furthermore, phospho-Smad2 signals were not found either in bulge keratinocytes or in melanocytes of *Col17a1*-null mice but were present in control mice (Figure 5H). These findings demonstrate that niche features, including the loss of TGF-β1/2 production, are defective in *Col17a1*-null HFSCs. We reported previously that *Tgfbr2* (TGF-β receptor II) conditional knockout in mice via a bitransgenic system causes mild hair graying with incomplete penetrance (73.3% within 10 months after birth) possibly because of incomplete CRE-mediated recombination (Nishimura et al., 2010). In this study, we found that *Tgfbr2* straight knockout mice (with a *Rag2*-null background for the inhibition of multiorgan autoimmunity) show a severe hair graying phenotype with 100% penetrance within 5–6 weeks of age (Figure 5I). Thus, these data suggest that defective TGF-β signaling in MSCs resulting from the loss of TGF-β production from HFSCs affects MSC maintenance in *Col17a1* mutant mice and that HFSC-derived TGF-β signaling mediates the niche function of HFSCs for MSC maintenance.

Human COL17A1-Mediated Rescue of HFSCs Normalizes Maintenance of MSCs in *Col17a1*-Null Mice

Finally, to address whether the defects in *Col17a1*-null HFSCs induce the ectopic differentiation and eventual depletion of MSCs in the bulge area, leading to hair graying, we studied the impact of the transgenic rescue of *Col17a1*-null mice and in particular the HFSC phenotype resulting from forced expression of human *COL17A1* under control of the *Keratin 14* (*Krt14*) promoter (Olasz et al., 2007). In these rescued mice, human COL17A1 expression was restricted to basal keratinocytes and not to the melanocyte lineage (Figure S6A). As shown in Figure 6A, the hair coat of these mice was quite similar to that of *Col17a1*$^{+/-}$ mice and did not show progressive hair depigmentation or hair loss at 6 months of age, or even at 1 year of age (data not shown), whereas control *Col17a1*-null mice demonstrated the hair graying and other typical changes described above. Interestingly, both the distribution and morphology of *Dct-lacZ*-expressing melanoblasts in the bulge area were normal in the *Col17a1*$^{-/-}$*; Krt14-hCOL17A1* rescued mice (Figure 6B). Furthermore, the aberrant expression of Ki67 and KRT1, downregulation of TGF-β1/2 expression, and inactivation of TGF-β signaling in bulge keratinocytes were all also normalized (Figures 6C and 6D; Figure S6B). These findings demonstrate the dual critical roles of COL17A1 in HFSCs for their maintenance and for providing a niche for MSC maintenance through HFSC-derived TGF-β signaling (Figure 7).

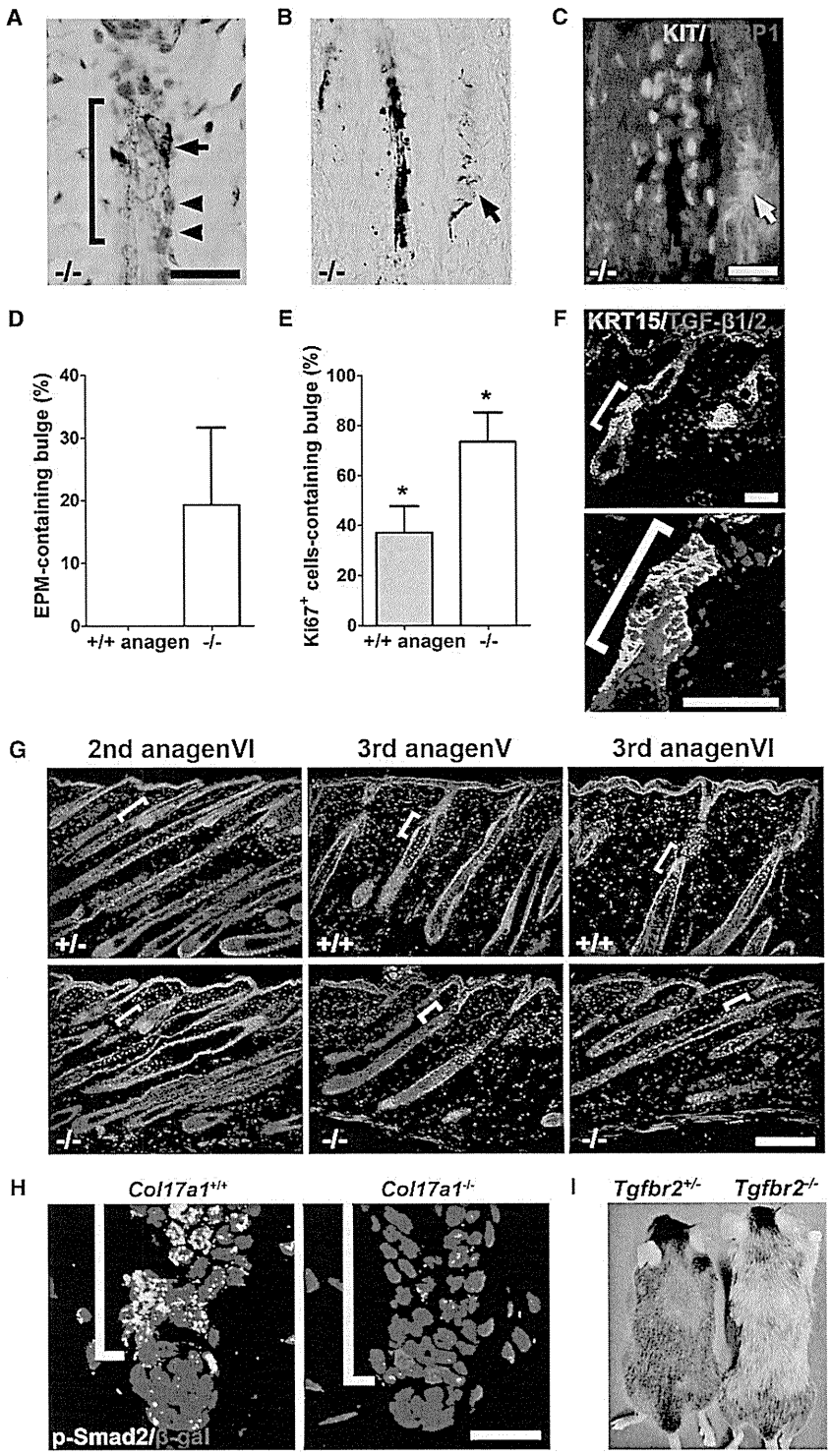

Figure 5. Ectopic Differentiation of MSCs in the Bulge Area with Diminished TGF-β Signaling Resulting from *Col17a1* Deficiency

(A–E) Ectopic differentiation of MSCs and surrounding keratinocytes in the bulge areas of *Col17a1*$^{-/-}$ follicles at 12 weeks of age. The bulge areas are demarcated by brackets. Ectopically pigmented melanocytes (A; arrow) are in direct contact with enlarged keratinocytes with large nuclei (A; arrowheads) in an anagen VI follicle; these ectopically pigmented melanocytes (arrow) are KIT^{+}/TYRP1^{+} cells with a dendritic morphology (B and C). Ectopically pigmented melanocytes were detected only in the bulge-subbulge area of *Col17a1*$^{-/-}$ follicles (D), and the proliferation of *Col17a1*$^{-/-}$ bulge keratinocytes at 12–13 weeks of age was abnormally accelerated compared with that of control anagen V follicles (E). *$p < 0.05$. Scale bars represent 30 μm in (A) and 20 μm in (B) and (C).

(F) Localization of TGF-β1/2 expression (red) in *Col17a1*$^{+/+}$ hair follicles. Plucked dorsal skins (4 days after hair plucking in telogen skin from 7-week-old *Col17a1*$^{+/+}$ mice) were used. KRT15-expressing keratinocytes (shown in green) express TGF-β1/2 (red). Scale bars represent 50 μm.

(G) *Col17a1*$^{-/-}$ mouse hair follicles from 5-week-old mice showed normal TGF-β1/2 expression patterns (left). However, at 8 weeks of age or later in *Col17a1*$^{-/-}$ mice, the TGF-β1/2 expression was downregulated (right and middle). Scale bar represents 200 μm.

(H) Phosphorylated Smad2 (shown in green) was not detected at 8 weeks in the *Col17a1*$^{-/-}$ hair follicle bulge. Dct-lacZ-expressing melanocytes in the bulge area are shown in red. Bulge areas are demarcated by brackets. Scale bar represents 20 μm.

(I) *Tgfbr2* straight knockout mice (*Tgfbr2* $^{-/-}$) (right) show severe hair graying phenotype at 6 weeks of age.

See also Figure S5.

DISCUSSION

Interactions between somatic stem cells and their surrounding niche microenvironment are critical for the establishment and maintenance of stem cell properties (Li and Xie, 2005; Moore and Lemischka, 2006). Although previous in vitro studies suggested some correlation in keratinocytes between integrin-mediated extracellular matrix adhesion and proliferation potential, in vivo ablation studies of major integrins in basal keratinocytes have not provided data on stem cell-specific depletion phenotypes (Dowling et al., 1996; Georges-Labouesse et al., 1996; Raghavan et al., 2000; van der Neut et al., 1996; Watt, 2002). In the present study, we demonstrated that COL17A1, a hemidesmosomal transmembrane collagen, is highly expressed in HFSCs within hair follicles and is required for the self-renewal of HFSCs. We found that *Col17a1* ablation in mice results in premature hair loss almost homogeneously over the entire body surface without showing any specific association